s Lib.

THE JOURNAL OF CHEMICAL PHYSICS

VOLUME 14 NUMBER 6

JUNE, 1946

Published by the

AMERICAN INSTITUTE OF PHYSICS

Incorporated

LANCASTER, PA., AND NEW YORK, N. Y.

The Journal of Chemical Physics

BOARD OF EDITORS

JOSEPH E. MAYER, *Editor*

Associate Editors

Term ending December 31, 1946

I. FANEUCHEN
PAUL J. FLORY
JOSEPH H. FRAZER
JOSEPH O. HIRSCHFELDER
W. F. LIBBY
WALTER H. STOCKMAYER

Term ending December 31, 1947

PAUL C. CROSS
RAYMOND M. FUOSS
JOHN G. KIRKWOOD
H. MARK
O. OLDENBERG
OSCAR K. RICE

Term ending December 31, 1948

CHARLES D. CORYELL
F. O. RICE
L. H. THOMAS
G. W. WHELAND
E. BRIGHT WILSON, JR.

THE JOURNAL OF CHEMICAL PHYSICS is published monthly by the American Institute of Physics. Its purpose is to bridge a gap between journals of physics and journals of chemistry. The artificial boundary between physics and chemistry has now been in actual fact completely eliminated, and a large and active group is engaged in research which is as much the one as the other. It is to this group that the Journal is rendering its principal service and makes its greatest appeal, both as a prompt and efficient medium for publication of research and as a convenient and carefully edited assemblage of pertinent information.

Notice for Contributors

Manuscripts for publication should be submitted to Joseph E. Mayer, Kent Chemical Laboratory, University of Chicago, Chicago 37, Illinois. Papers are published in English only. To be acceptable for publication manuscript should be original typewritten copy (not carbon copy) either double or triple spaced, with wide margins. References should appear as footnotes only and should be numbered consecutively to avoid repetition. References should include author's name, journal, volume number, page number, and year and should be listed in the order given here. Attention should be given to captions for tables and legends for figures. These in all cases should be complete in themselves so as to make the data intelligible to the reader without consulting the text of the article.

Special care should be given to mathematical expressions. The very simplest formulas only should be typewritten and all others carefully written in with pen and ink. Fractional exponents should be used to avoid root signs everywhere. Extra symbols should be used to avoid complicated exponents. The solidus (/) should be used wherever possible for fractions.

All illustrations should accompany manuscript and should always be referred to in the text. Line drawings must be made with India ink on plain white paper or on tracing cloth. Coordinate paper is not desirable, but if used must be blue-lined with all coordinates to be reproduced drawn with India ink. Lettering should be of sufficient size to be legible after reduction.

Proof and all correspondence concerning papers in the process of publication should be addressed to the Publications Manager, American Institute of Physics, 57 East 55 Street, New York 22, New York.

Subscription Price

The United States and Possessions, Canada and Mexico	$10.00
Elsewhere	11.00

Back Numbers

Complete set: Vol. 1, 1933—Vol. 13, 1945 ..... **$130.00**
Yearly rate: $11.00.
Single copies: $1.00 each.

Subscriptions and orders for single copies should be addressed to Prince and Lemon Streets, Lancaster, Pennsylvania, or to the American Institute of Physics, 57 East 55 Street, New York 22, New York.

Changes of address should be sent to the Business Manager, American Institute of Physics.

The Journal of Chemical Physics is published monthly at Prince and Lemon Streets, Lancaster, Pennsylvania.

Entered as second-class matter December 30, 1932, at the Post Office at Lancaster, Pa., under the Act of August 24, 1912. Acceptance for mailing at special rate of postage, provided for in the Act of February 28, 1925, embodied in paragraph 4, Section 538, P. L. & R., authorized February 4, 1933.

THE JOURNAL
OF
CHEMICAL PHYSICS

VOLUME 14, NUMBER 6 JUNE, 1946

Thallous Sulfide Photo-Conductive Cells

I. Experimental Investigation*

A. VON HIPPEL, F. G. CHESLEY, H. S. DENMARK,** P. B. ULIN, AND E. S. RITTNER
Laboratory for Insulation Research, Massachusetts Institute of Technology, Cambridge, Massachusetts

(Received March 4, 1946)

An experimental study of thallous sulfide photo-conductive cells is presented. It includes an investigation of the sensitizing oxidation reaction; cell characteristics as function of voltage, temperature, light intensity, wave-length, modulating frequency, and composition; measurements of thermoeffect and optical absorption; x-ray and electron diffraction studies, and an examination of the photo-response to light flashes of very short duration. A theoretical discussion will be given as Part II in a subsequent paper.

INTRODUCTION

THE photo-sensitivity of oxidized thallous sulfide was discovered by T. W. Case in 1917. Since his initial work[1] some progress has been made in improving the stability and response of this photo-conductive cell[2,3] as a result of empirically developed[4–6] and undisclosed[2] processes of manufacture. More recently the photo-cell, as further developed by R. J. Cashman,[7] has become of importance in this country for war communication systems, but its usefulness at present is limited by lack of appreciable sensitivity above a wave-length of 1.2μ and by poor frequency response.[8] A fundamental study was therefore undertaken with the objective of gaining insight into the photoelectric mechanism, as such knowledge should be of considerable assistance in understanding and improving the cell properties.

I. PREPARATION OF THALLOUS SULFIDE

Three batches of thallous sulfide were prepared* by two different methods. In the first of these, thallous sulfide was precipitated by means of hydrogen sulfide from an ammoniacal solution containing thrice recrystallized thallous sulfate. The deposit was washed, dried, and fused in vacuum, yielding a product of reasonable purity (see analysis of sample No. 1 in Table I). However, owing to unavoidable oxidation in the course of handling the finely divided precipitate under atmospheric conditions, this batch of material was used only for exploratory experiments.

* This research was carried out under contract OEMsr-1036 with Division 16, Section 16.4, of the National Defense Research Committee and completed in June, 1945. Publication has been delayed because of the war.

** Deceased.

[1] T. W. Case, Phys. Rev. **15**, 289 (1920).
[2] R. Sewig, Zeits. f. tech. Physik **11**, 269 (1930).
[3] W. Leo and C. Mueller, Physik. Zeits. **36**, 113 (1935).
[4] Q. Majorana and G. Tedesco, Atti accad. Lincei **8**, 9 (1928).
[5] F. Michelssen, Zeits. f. tech. Physik **11**, 511 (1930).
[6] A. A. Sivkov, J. Tech. Phys. U.S.S.R. **8**, 11 (1938).
[7] R. J. Cashman, N.D.R.C. Report No. 16.4–6 (1943).
[8] W. L. Hole and R. J. Cashman, N.D.R.C. Report No. 16.4–7 (1943).

* The preparation of the material was the work of M. C. Bloom and J. P. Levy.

TABLE I. Spectrographic analyses.

Material	Impurities, parts per million									
	Al	Cu	Fe	Ca	Ag	Na	Mg	Ni	Pb	B
Tl_2S No. 1 (pptn.)	6	4	4	25	—	40	10	5	35	—
Tl_2S No. 2 (synthesis)	0.5	2	0.5	0.5	<.04	.04	.1	<1	>100	—
Tl_2S No. 3 (synthesis)	1	8	<1	1	<.05	<1	<.3	<2	3	<2

The other batches were prepared by reacting stoichiometric quantities of thallium and sulfur at elevated temperatures in evacuated quartz apparatus. The sulfur was purified by the method of Bacon and Fanelli.[9] In the case of sample No. 2, C.P. thallium metal, which had been melted and strained in vacuum to remove oxide, was employed. A more elaborate procedure was followed in purifying the metal in the preparation of sample No. 3, consisting of three successive fractional crystallizations of thallous sulfate, cathodic deposition of thallium from the saturated sulfate solution acidified with dilute sulfuric acid, washing, drying, and melting and straining in vacuum. This latter sample was also stirred with nitrogen during the reaction to assure homogeneity throughout the melt.

Table I summarizes the spectrographic analyses of the different thallous sulfide products.

Sample No. 2 was employed in the majority of the experiments described in this paper. Sample No. 3, available only in the later stages of the research, served to demonstrate that the photosensitivity of thallous sulfide originates from its oxygen content and not from accidental impurities.

II. THERMAL STABILITY OF THALLOUS SULFIDE

Inasmuch as thallous sulfide is evaporated in vacuum as the first step in preparing photo-cells, its thermal stability is of great importance. From known values of free energy content and heat of formation, calculation* was made of the change in free energy attending the change in state:

$$Tl_2S \text{ (solid)} \rightarrow 2 \text{ Tl (liquid)} + \frac{1}{X} S_x \text{ (gas, } 10^{-6} \text{ mm) at 450°C.}$$

The calculation assumes that S_x is made up of an approximately equal mixture of S_6 and S_8 molecules. ΔF is positive in sign and amounts to about 20,000 calories, indicating that thallous sulfide will not spontaneously decompose into its elements under the above mentioned conditions.

An attempt was made to confirm this conclusion by heating a thallous sulfide layer, evaporated in the usual type of cell (see Section IV), for several hours in vacuum to progressively higher temperatures. After each heating period the cell was quenched and measurement made of its conductivity, which certainly should be affected by decomposition. No appreciable change in conductivity resulted until at about 400°C the experiment came to an end because the layer sublimed off the grid electrodes.

III. OXIDATION REACTION

Thallous sulfide is photo-sensitized by oxidation. A study of the oxidation reaction at 250°C and 350°C by gas absorption, and x-ray and electron diffraction methods was therefore undertaken to identify the reaction products.

A. Gas Absorption Method

It is a prerequisite of accurate gas absorption measurements that the system be of small volume so as to maximize the change in pressure accompanying the reaction. The essential portion of the apparatus employed is sketched in Fig. 1. Volume B between the stopcocks C and D was calibrated with water before sealing to the vacuum system ($B \sim 45$ cm³). The small volume of the Pirani gauge,* P, was estimated from the bore of the tubing employed. The reaction vessel comprising the major portion of volume A ($A \sim 45$ cm²) was made from Nonex glass tubing of 30 mm o.d.

For each reaction vessel, volume A was cali-

[9] R. F. Bacon and R. Fanelli, Ind. Eng. Chem. **34**, 1043 (1942).

* Calculation performed by J. H. Schulman.

* A description of a more rugged model of this gauge, which is capable of measuring pressures up to 15 mm, will be published elsewhere.

brated by filling *A* and *B* to a predetermined pressure, evacuating *B*, reconnecting *A* and *B*, and establishing the resulting pressure. A weighed amount of thallous sulfide (14.5±1 mg in the usual case, known to ±0.1 mg) was then introduced into the reaction vessel, the system evacuated, the vessel outgassed at 400°C for an hour, and the entire sample evaporated by heating with a Bunsen burner (film thickness about 5000A). To initiate the reaction, the vessel was heated by an oven to the desired temperature, tap *D* closed, oxygen at known temperature introduced into volume *B* to the desired starting pressure, and tap *D* opened. The progress of the reaction was measured by observing the pressure as a function of time at the constant temperature for a period up to twenty hours. The reaction vessel was then quenched by an air blast and the pressure re-measured at room temperature with the whole system in temperature equilibrium. This completes the data required to calculate the composition of the oxidized layer.

Visual observation of thallous sulfide layers oxidized to varying degrees reveals that the photo-cell material consists of two phases: a grayish-black (photo-sensitive) substance and a bright yellow (insulating) material. With progressing oxidation the quantity of the yellow phase increases; and at a composition approximated by 1 mole O_2 per mole Tl_2S, the black phase completely disappears.

The existence of these phases, and of only these two phases, was confirmed by the x-ray and electron diffraction studies reported below.

B. X-Ray Diffraction Study

X-ray powder photographs were taken of a number of photo-sensitive layers carefully removed from the cells in a nitrogen atmosphere and sealed in small glass capillaries. A phase found to be present in all sensitive cells gave rise to a diffraction pattern* correlating satisfactorily with the structure of Tl_2S proposed by Ketelaar and Gorter.[10] Usually a second (yellow) phase was observed in addition. The diagram in Fig. 2 shows the positions and relative intensities of diffraction lines from patterns obtained with pure Tl_2S, with a typical photo-cell sample and with the yellow material from a "completely" oxidized layer.

Inasmuch as the photo-sensitive phase possesses the same structure as thallous sulfide, it is probably safe to conclude that the former represents a solid solution of oxygen in Tl_2S. The change in lattice constants with composition usually observed in solid solutions, if present, could not be detected in the present case because the small crystallites in the evaporated layers produced diffuse lines in the high θ region and prevented accurate measurements.

The interplanar spacings calculated from the diffraction photograph of the yellow phase indicate a face-centered cubic lattice with a cell edge of 10.77A. Since this phase has a structure differing from any of the known structures of thallium compounds and since its composition is about 1 mole O_2/mole Tl_2S, it may be identified as the compound Tl_2SO_2.[11] This substance proved quite stable; it cannot be decomposed at a reasonably rapid rate by heating in vacuum unless a temperature high enough to sublime the material is employed. The gray condensate resulting consists of a mixture of the Tl_2S and Tl_2SO_2 phases.

In passing, it may be noted that no changes in structure were observed on heating thallous sulfide up to 385°C. From the displacement of the

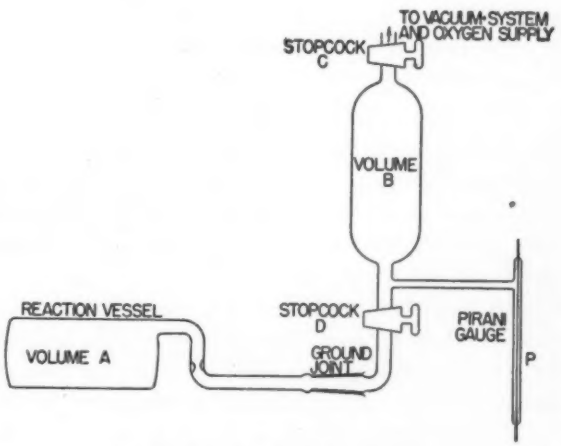

FIG. 1. Reaction vessel, system *A*.

* This same pattern was obtained with our fused samples of thallous sulfide and with unoxidized evaporated layers.

[10] J. A. A. Ketelaar and E. W. Gorter, Zeits. f. Krist. **101**, 367 (1939).

[11] Reference to the existence of this compound has been made by I. I. Iskoldsky, Mineralnoje Syrye No. 4, 404 (1931).

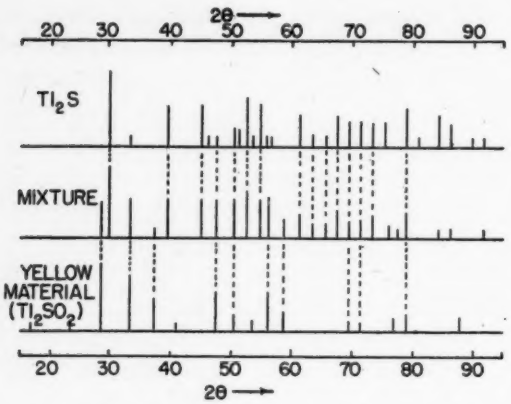

FIG. 2. X-ray diffraction patterns.

(0006) reflection in the x-ray diffraction patterns it was possible to determine the linear coefficient of thermal expansion in the direction of the "c" axis. The value, $\alpha = 34 \times 10^{-6}$ (20–385°C), does not differ appreciably from that of thallium metal, $\alpha = 30.3 \times 10^{-6}$.

C. Electron Diffraction Study

For the electron diffraction investigation a cell was produced in the diffraction apparatus itself for a study at grazing incidence. On account of the relatively low conductivity of the thallous sulfide, the diffraction specimen charged up if not prepared on a conducting surface. The sample prepared on a glass slide consisted of two parts: a section on aquadag from which the diffraction studies were made and immediately adjacent to it a photo-cell section with its standard gridwork (see Section IV). Thallous sulfide was vacuum evaporated from a small crucible onto the surface of this slide and also onto Formvar Films of thickness about 100A for transmission studies. Examination of the diffraction patterns obtained (see Fig. 3, $a+b$-transmission patterns, c-reflection pattern) show the crystals of thallium sulfide to be arranged with their "c" axis preferably oriented in a direction perpendicular to the receiving surface. The slide was then heated for twenty minutes at 250°C at an oxygen pressure of 2 mm, resulting in the development of an appreciable photo-sensitivity. The electron diffraction pattern from the sensitive surface is shown in Fig. 4a; the interplanar spacings check those from the unoxidized Tl_2S pattern. In addition, it may be noted that the original orientation persists and that the crystallites have grown in size. However, the pattern is considerably more diffuse than that from the unoxidized surface and indicates that the structure has probably been disrupted by solid solution of some oxygen. More complete oxidation produced the pattern shown in Fig. 4b; the interplanar spacings check the x-ray data from the yellow material. Hence, the electron diffraction data lead to the same conclusions as those suggested by the x-ray diffraction results.

IV. PREPARATION OF CELLS

Cells prepared by a single oxidation treatment at 250° and 350°C were investigated with the purpose of obtaining data on dark resistance and photo-sensitivity as a function of oxygen content. In addition, the reproducibility of the characteristics of photo-cells prepared under closely identical conditions was studied.

A. Methods

Two vacuum systems of different design were employed in the preparation of these cells. The first one, system A, has already been described in Section III A and was used with the following changes. The reaction vessel was furnished with sealed-in tungsten electrodes and an aquadag gridwork as shown in Fig. 5.* The gridwork covered an effective area of $1'' \times 1''$ with 16 lines per inch. Pretreatment of the cell blank consisted of a heat treatment in air for several minutes at 400°C followed by a heating in a vacuum for one hour at 500°C. The introduction of sample, outgassing, evaporation, and oxidation were carried out by a procedure similar to that outlined in Section III A. After quenching, the resistance and photo-sensitivity of the cell were determined; the oxygen was pumped out, which did not affect the sensitivity; and the cell was sealed off. Since its properties changed rapidly with time for a few days, the resistance and sensitivity increasing in general, final measurements were postponed until the characteristics had stabilized.

The essential features of the second system, system B, which was designed to operate with a large volume (2 liters) of oxygen at pressures of the order of those employed in the commercial

* After a design of R. J. Cashman.

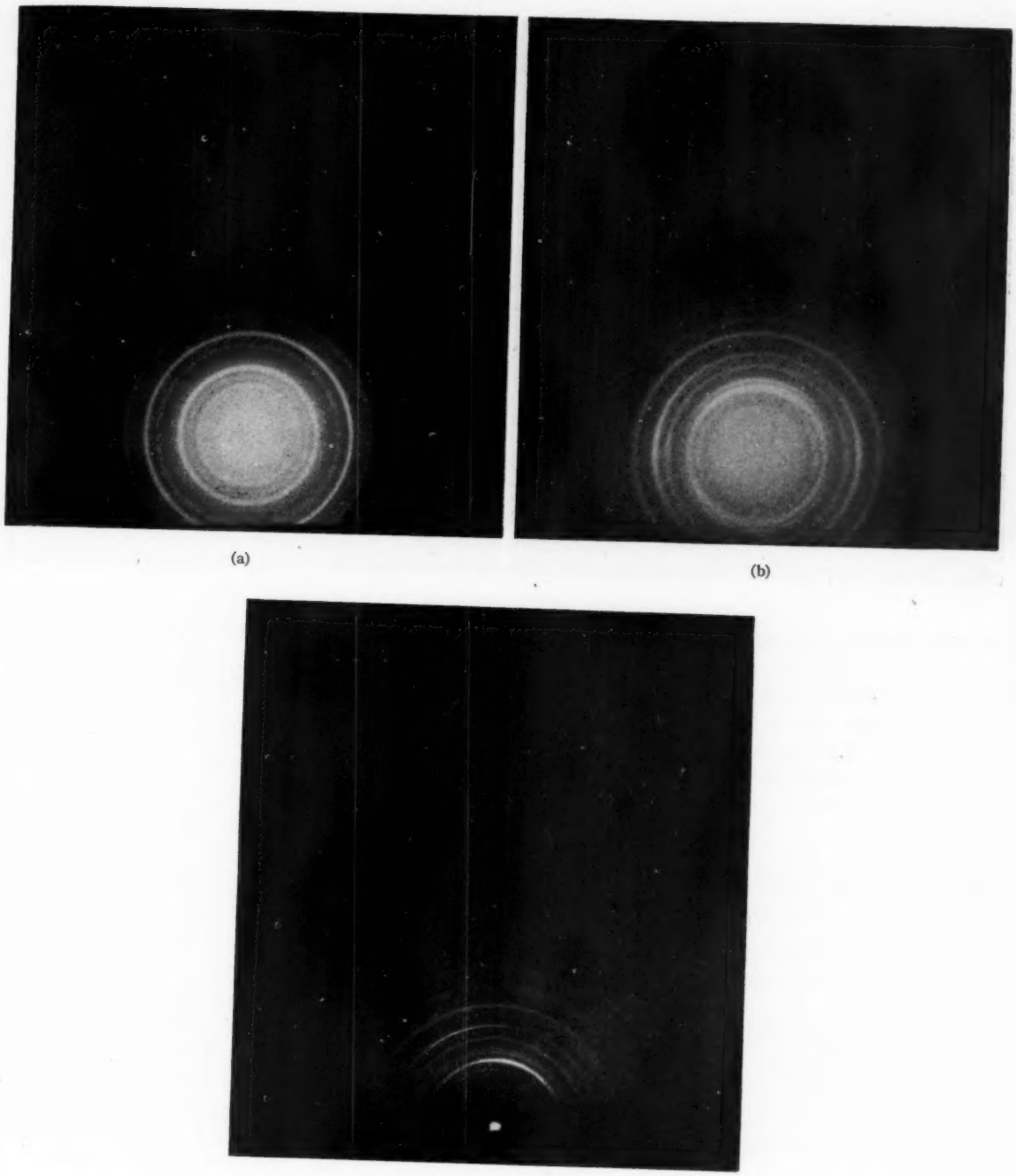

(a) (b)

(c)

FIG. 3. Electron diffraction patterns of thallous sulfide:
(a) electron beam ⊥ to Tl_2S film
(b) Tl_2S film inclined 45° to electron beam } transmission
(c) electron beam at grazing incidence to Tl_2S surface.

process,[12] are shown in Fig. 6. The preparation of cells was carried through as before with the minor exceptions that the volume of the cell blank, *ca.* 40 cc, was not accurately determined, that oxygen was introduced prior to heating, and that the reaction was initiated by covering the cell

[12] C. W. Hewlett, J. J. FitzPatrick, H. T. Wrobel, N.D.R.C. Report 16.4–39 (1945).

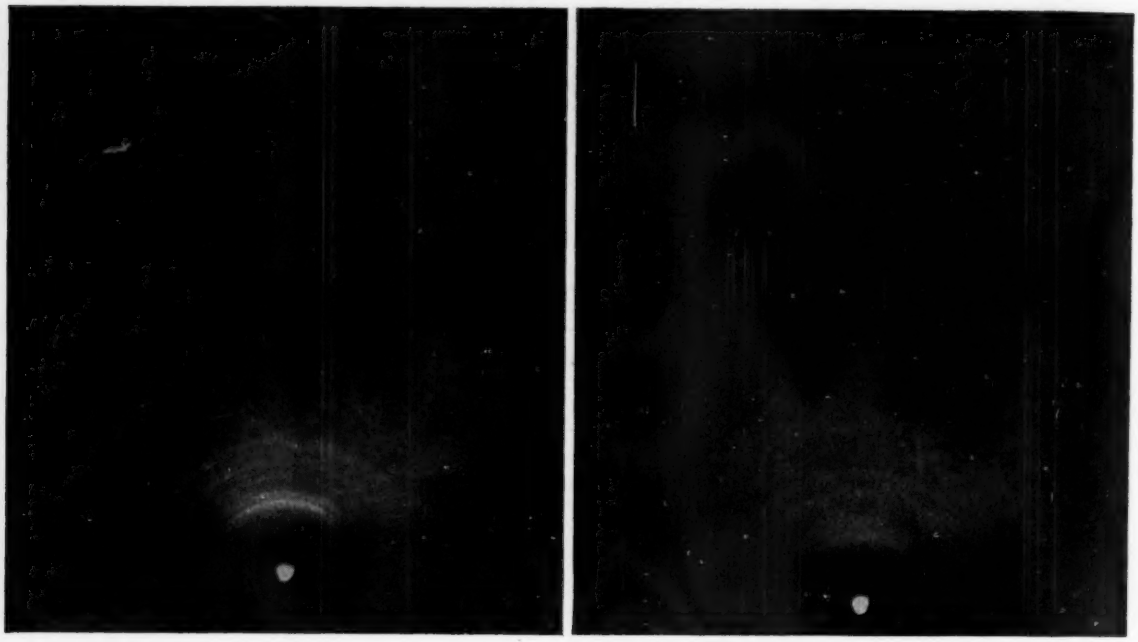

(a) (b)

FIG. 4. Electron diffraction patterns of oxidized thallous sulfide layers: (a) Tl_2S phase, (b) Tl_2SO_2 phase.

with the hot oven. The oxidation was allowed to proceed for about twenty hours; at the end of this period the cell was quenched, sealed, and measured as described above. The residual pressure was also determined to permit an estimation of oxygen content.*

B. Resistance and Photo-Sensitivity as Function of Oxidation

Data on dark resistance, thermal activation energy, U, and photo-sensitivity of cells, prepared from sample No. 2 in systems A and B by oxidation at 250°C, as a function of the composition of the oxidized layer are tabulated in Table II and similar data at 350°C for system B are shown in Table III.**

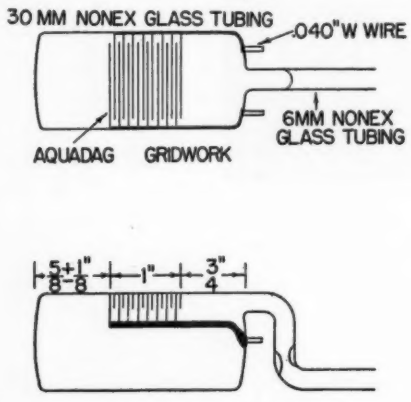

FIG. 5. Cell blank.

For the cells prepared at 250°C there is no discernable relation between thermal activation energy (see Eq. (4)) and oxygen content; however, the dark resistance increases with oxidation until quite sensitive cells are obtained. Beyond this point correlation between resistance and composition is obviated by the large fluctuations in the value of the dark resistance of cells prepared by the same procedure.

Table II shows, in addition, that the minimum amount of oxygen required for producing a sensitive cell varies with the range of pressures employed. Although under the conditions of system A about 0.3 mole O_2/mole Tl_2S is required, in system B about 0.1 mole O_2/mole Tl_2S suffices. This apparently results from the simultaneous or successive occurrence of two oxidation products, the relative amounts of which vary in accordance with operating conditions. The absorption of still more oxygen does not improve

* We are indebted to R. B. Speed for the preparation of cells in system B.

** See Section V for details on measurements, definitions of terms, and references.

the photo-conductivity further but converts more of the thallous sulfide phase into Tl_2SO_2. Highly sensitive cells can therefore be made at 250°C even though the operating pressure varies over wide limits. The variations in sensitivity of cells prepared by the same process are appreciable but not as extreme as the fluctuations in the resistance.

In the case of the cells prepared at 350°C, the compositions are higher in oxygen than the corresponding ones attained at 250°C owing to the increased rate of reaction at the higher temperature. The electrical characteristics do not differ fundamentally, however, in the two sets of cells.

V. CHARACTERISTICS OF THALLOUS SULFIDE PHOTO-CONDUCTIVE CELLS

A determination of whether the photo-sensitivity of the cell represents a primary or secondary photo-effect is of paramount importance. The sluggishness of the cell,[1,13,14] its strong temperature dependence[1,13] and poor frequency response[2] indicate a secondary type. In addition, Runge and Sewig[15] have concluded from their measurements that light creates disturbance centers which decay exponentially with time. An unequivocal decision can be obtained by a determination of the quantum yield. While a primary photo-effect makes use only of the charge carriers liberated by the absorption of light quanta and is normally limited to a maximum yield of one electron per quantum absorbed, a secondary photo-effect changes the conductivity of the material and quantum yields far exceeding unity may result.

The characteristics of representative Cashman cells* were investigated as a function of voltage, temperature, light intensity, and wave-length.

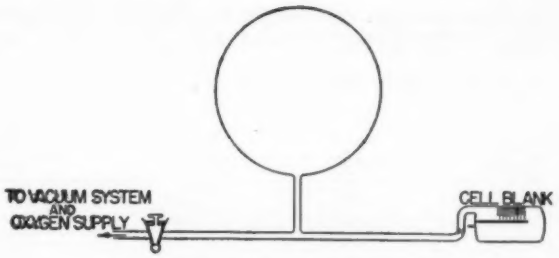

FIG. 6. Reaction vessel, system *B*.

TABLE II. Resistance and photo-sensitivity *vs.* oxidation, 250°C.

System	Cell No.	Composition, mole O_2/ mole Tl_2S	Initial pressure, mm	Dark resistance, megohms	Thermal activation energy, electron volts	White light sensitivity: $\Delta I/I_0$ at .023 hololumens per in.[2]	White light sensitivity: Response to 90-cycle modulated light, signal: noise with infra-red transmitting filter,[a] db
A	2–7	0[b]	—	.0075–.022	.59[c]	0	—
	5	0.119	1.50	.011	.48	.01	0
	4	0.251	2.92	6.1	.62	2.6	27
	6	0.339	4.99	28	.47	22	66
	2	0.578	6.56	225	.61	30	40
	7	0.760	8.48	45	.46	19	57
	3	1[d]	12.65	∞	—	0	—
B	—[b]	0	—	.022–.11	.54[c]	0	—
	72	.06	.025	0.55	.52	0.25	24
	68	.13	.051	187	.79	55	62
	56, 58, 60, 64, 66, 86	.16	.09	1.7–204	.77[e]	19–198	52–62
	24, 40, 50, 52, 54, 84	.39	.62	2.5–55	.70[f]	18–44	58–67
	70	.49	1.92	37	.41	35	61

[a] Without filter S/N ratios are about 12 db higher.
[b] After initial evaporation.
[c] Owing to the high conductivity of the unoxidized material, the resistance of the gridwork is not negligible compared to that of a layer of standard thickness; hence, a much thinner layer was employed.
[d] Sample completely yellow.
[e] Cell No. 64.
[f] Cell No. 54.

[13] W. W. Coblentz, Bur. Stand. J. Research **16**, 254 (1920).
[14] I. Kaplan, J. Opt. Soc. Am. **14**, 253 (1927).
[15] I. Runge and R. Sewig, Zeits. f. Physik **62**, 726 (1930).
* The gridwork covered an effective area of $\frac{3}{4}'' \times \frac{3}{4}''$ with a spacing of 1/30″ between adjacent lines.

TABLE III. Resistance and photo-sensitivity *vs.* oxidation, 350°C.

Sample	Cell No.	Composition, mole O_2/ mole Tl_2S	Initial pressure, mm	Dark resistance, megohms	White light sensitivity $\Delta I/I_0$ at .023 hololumens/in.²	White light sensitivity Response to 90-cycle modulated light, signal: noise with infra-red transmitting filter, db
9C*	138	0.21	0.10	72.5	5.6	48
9C	168	0.30	0.18	10.5	1.7	54
9C	166	0.36	0.18	140	25.8	46
9C	136	0.38	0.16	1.05	33.5	50
2	116	0.16	0.066	0.15	6.8	51
2	114	0.69	0.53	840	25.8	48

* Material employed in the commercial process.

A. Apparatus

Monochromatic** radiation was obtained by the use of a Gaertner instrument (L234-HT) with quartz optics, the output of which was focused by a mirror system alternately on the test cell or on a thermocouple.

For determining its temperature dependence, the cell was mounted in an electrically heated housing or in a double-walled container thermostated by circulating liquids.

Three tungsten lamps, covering a wide range of light intensities and calibrated in terms of microwatts as well as microhololumens*** were employed in "white light" measurements. Tests with square-wave modulated light of one microhololumen peak (without filter) were carried out on the standard instrument developed at the University of Michigan.[16,17]

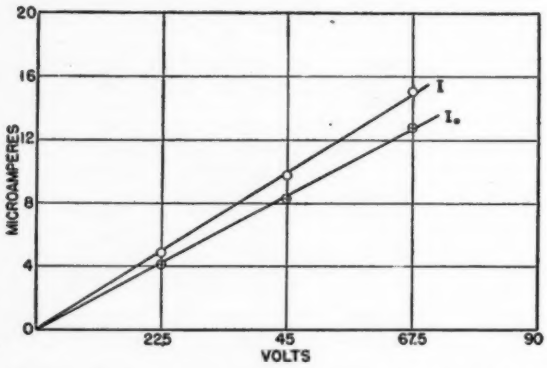

FIG. 7. Dark current, I_0 and total current, I, obtained with illumination as function of applied voltage ($\lambda=0.8\mu$; $F=0.5$ microwatts).

B. Effect of Applied Voltage

For a thallous sulfide cell the dark current, I_0, and the current, I, obtained under illumination are proportional to the voltage applied, V, at constant temperature (Fig. 7); that is

$$I_0 = VG_0 = V/R_0, \tag{1}$$

$$I = I_0 + \Delta I = VG$$

$$= V(G_0+\Delta G) = \frac{V}{R} = \frac{V}{R_0-\Delta R}, \tag{2}$$

where R_0 is the dark resistance, R the resistance under illumination, and G_0 and G the corresponding conductances.

It follows from Eqs. (1) and (2) that the cell

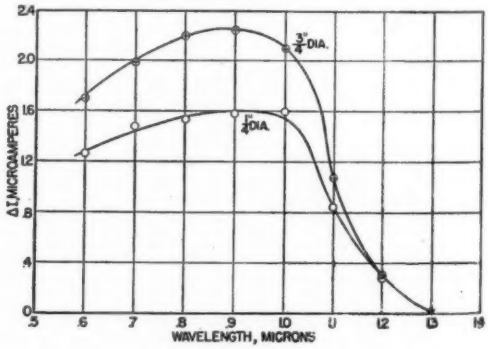

FIG. 8. Effect of spot size on photo-current for constant light input. ($R_0=5.4$ meg.; $V=22.5$ v; $F=1$ microwatt.)

** $\Delta\lambda\sim150$A.

*** One hololumen is that radiant flux of all wavelengths which has the spectral distribution characteristic of a tungsten lamp at color temperature 2848°K, and which, evaluated as visible light, equals one lumen. (See N.D.R.C. Report No. 16.4–10 (1943) by G. A. Van Lear, Jr.)

[16] W. L. Hole, N.D.R.C. Report No. 16.4—Special No. 9 (1944).

[17] L. N. Holland, N.D.R.C. Report No. 16.4—Special No. 6 (1944).

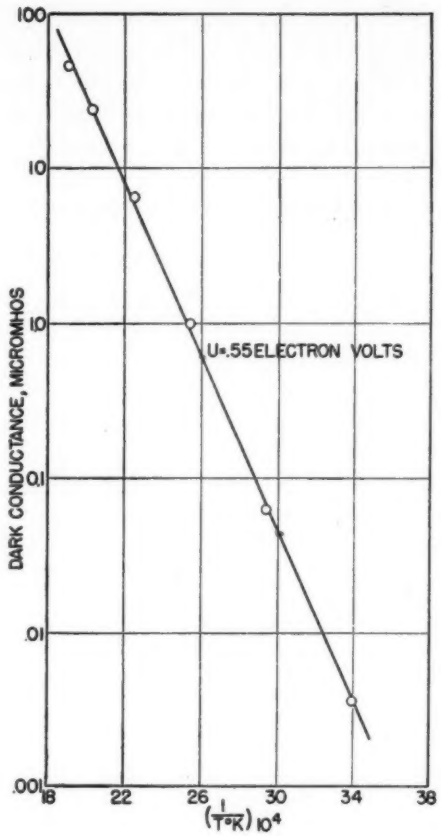

FIG. 9. Temperature dependence of the dark conductance.

sensitivity can be characterized independently of V by the ratios

$$\Delta I/I_0=\Delta G/G_0=\Delta R/R. \tag{3}$$

In addition, presentation of data in this form permits comparisons of sensitivity between cells of different area and grid spacing.

In order to utilize the above equations, it is essential that the photo-sensitive area of the cell be uniformly and completely illuminated. These conditions have only been approximated in measurements requiring the use of the monochromator by employing a spot size of diameter equal to the length of the side of the square sensitive surface. The effect of spot size on cell response for constant light input is illustrated by Fig. 8.

C. Dark Current and White Light Response

The temperature dependence of the dark conductance of oxidized thallous sulfide is typical of that of a semiconductor, G_0 decreasing exponentially with the reciprocal of the absolute temperature over a wide range (Fig. 9, Eq. (4)).

$$G_0=ae^{-U/kT}, \tag{4}$$

a = constant, U = activation energy.

Owing to the high temperature coefficient of the dark current, the accuracy of light response measurements is limited at very low and very high light intensities; but, as is evident from Fig. 10, only at very low levels of illumination does the photo-current increase proportionally to the light input. At higher light intensities the response deviates considerably from linearity. This behavior explains the previously noted observation (Fig. 8) that the output decreases when the light is concentrated on a smaller spot.

D. Spectral Response and Quantum Yield

The spectral response characteristic of the thallous sulfide cell (Fig. 11) varies with the illumination level because of the non-linearity of the cell. In addition to the photo-current, ΔI, the quantum yield, η, is plotted in Fig. 11, assuming that every incident light quantum is absorbed and contributes to the photo-effect:

$$\eta=\frac{\text{photo-electrons}}{\text{incident quanta}}=\frac{(1.24)(\Delta I)}{(\lambda)(F)}. \tag{5}$$

(ΔI = photo-current in μ amp., F = light input in μ watts, λ = wave-length in microns). Because of this assumption, the calculated quantum yield will be lower than the true yield; nevertheless, the former surpasses unity by a large margin.

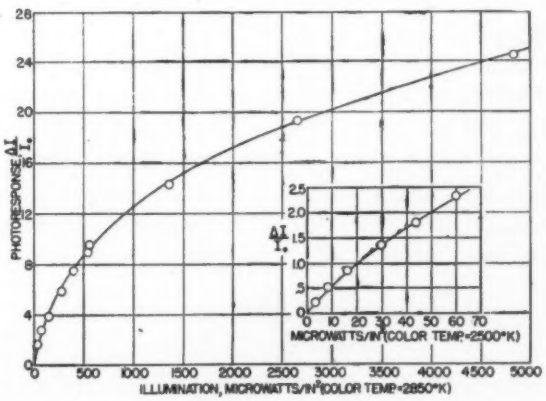

FIG. 10. White light response as a function of illumination.

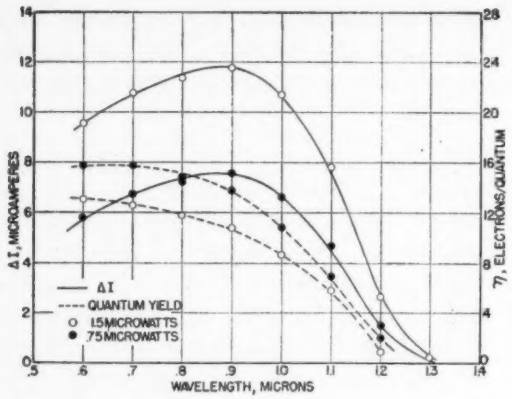

FIG. 11. Photo-current and quantum yield as function of wave-length for two light intensities. ($R_0=2.5$ meg.; $V=22.5$ v.)

This result establishes beyond question that the photo-currents observed in thallous sulfide cells are the result of a secondary photo-effect.

Plots of light response *vs.* intensity for different wave-lengths (Fig. 12) are similar in shape and, in fact, can be combined into a single curve by multiplying the μ-watt scale of each plot by a characteristic factor, a. For example, in Fig. 13 all curves have been converted into the 0.9μ characteristic by employing the a factors tabulated in the figure. It appears that a plot of the different a factors against wave-length represents a relative spectral sensitivity curve for constant light current output.

$$a=\frac{\eta_\mu\lambda_\mu}{\eta_{0.9}\lambda_{0.9}}. \qquad (6)$$

This curve also corresponds to the relative spectral sensitivity curve that would be obtained at very low illumination levels within the linearity range.

Similarly, all plots of light response *vs.* intensity for different temperatures and for a given wave-length (Fig. 14) can be combined into a single one by multiplying the μ-watt scale by factors b (Fig. 15). Again a plot of b against temperature indicates how the response varies with temperature for a constant light current output.

VI. THERMOELECTRIC STUDIES ON THALLOUS SULFIDE

The type of electronic conduction prevailing in semiconductors can be determined from the sign of the thermal e.m.f. Since the mobile charge carriers stream from the hot to the cold junction, excess conductivity charges the cold junction negative, while the migration of holes produces the opposite polarity.

A. Apparatus and Procedure

Measurements* of the thermovoltage coefficient were made on a number of thin films of thallous sulfide in various stages of oxidation. Figure 16 shows the special type of cell used in these measurements. The two tungsten electrodes were ground flat and sealed into the Pyrex bulb through glass arms, which could be filled during the experiments with liquids of the desired temperature difference (~60°C). The faces of the electrodes were covered with aquadag, which was subjected to the standard outgassing procedure before thallous sulfide was evaporated onto the

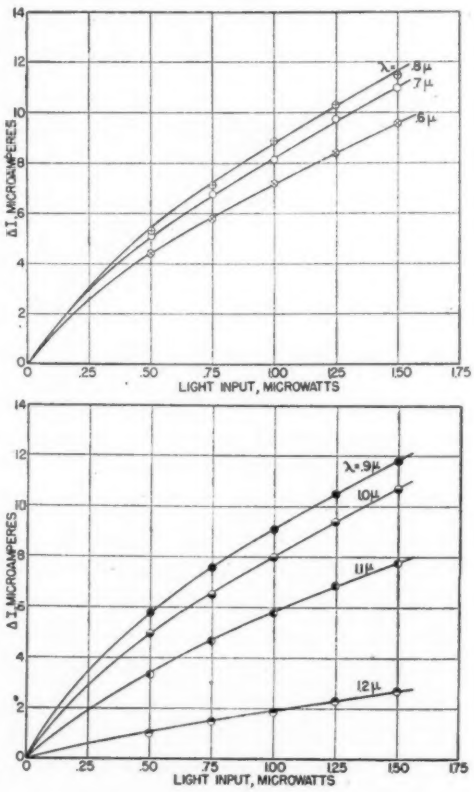

FIG. 12. Photo-response *vs.* light intensity and wave-length. ($R_0=2.5$ meg.; $V=22.5$ v.)

* The thermoelectric study was begun and the majority of these measurements were made by G. Oster, the remainder by R. B. Speed.

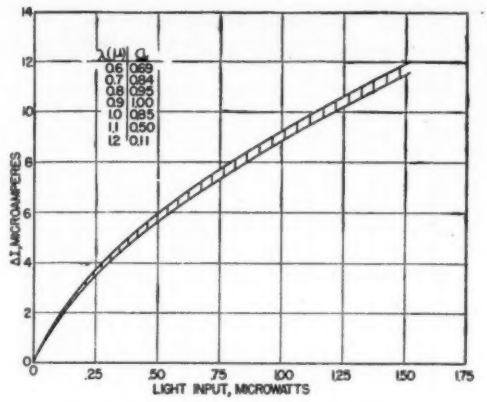

FIG. 13. Conversion of wave-length curves into the 0.9μ characteristic.

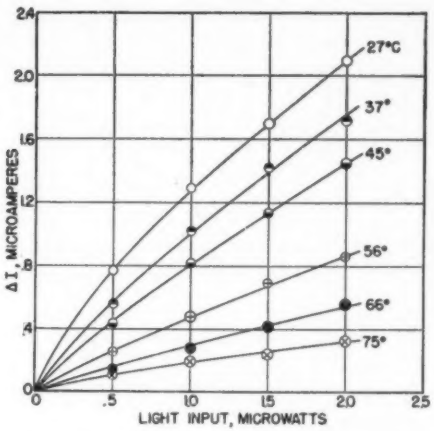

FIG. 14. Effect of temperature on photo-response. ($\lambda = 0.8\ \mu$; $V = 22.5$ v.)

upper half of the glass bulb. Thermovoltages were measured by means of a feedback amplifier of high input impedance.[18]

B. Results

Thallous sulfide sample No. 1, which was known to be slightly pre-oxidized (Section I), exhibited defect conductivity after evaporation and the sign of the thermal e.m.f. did not change on further oxidation. However, sample No. 2, which was completely free of oxygen, manifested excess conductivity after evaporation. With increasing oxidation of this sample the conductivity fell, the photo-sensitivity rose, and the thermovoltage went through zero and reversed sign as is shown in Fig. 17. Defect conductivity is represented in the figure by a positive sign of the thermal-e.m.f. coefficient.

A minimum in the conductivity characteristic did not accompany the change in sign of the thermo-e.m.f., in contradistinction to a case like PbS[19] where the material is an insulator at the stoichiometric composition and a defect or excess conductor in the presence of a defect or excess of the metallic constituent. Hence, if sample No. 2 does not contain an excess of either of its constituent elements, the data seem to indicate that thallous sulfide is both an excess and defect conductor and that oxidation reduces the originally dominating excess conductivity to a higher degree than the hole conductivity, thus producing a reversal of sign.

Illumination of an oxidized layer resulted in a slight increase in the magnitude of the positive thermovoltage, indicating that light increases the defect conductivity of the material.

Thermal e.m.f. measurements have previously been made by Hochberg and Sominski[20] on thallium sulfide samples subjected to a variety of heat treatments in air. We agree with these authors that high resistant Tl_2S shows defect and low resistant material shows excess conductivity; but their conclusion that pure Tl_2S is a hole conductor, changing to an excess conductor on oxidation, is contrary to our findings.

VII. TRANSMISSION AND REFLECTANCE MEASUREMENTS ON THALLOUS SULFIDE LAYERS

Transmission measurements between 3000 and 8500A* were made on several evaporated films of thallous sulfide prepared in cells of normal construction but lacking gridworks. Typical data obtained on very thin films are shown in Fig. 18. It is apparent that the absorption increases at shorter wave-lengths.

Measurements of transmission and reflectance between 4000 and 7000A** were made using a special absorption cell, fabricated from "Precision Bore" tubing of square cross section and containing a Tl_2S layer of standard thickness (5000A). The transmission proved to be less than

[18] S. Roberts, Rev. Sci. Inst. **10**, 181 (1939).
[19] H. Hintenberger, Zeits. f. Physik **119**, 1 (1942).
[20] B. M. Hochberg and M. S. Sominski, Physik. Zeits. Sowjetunion **13**, 212 (1938).

* A Hilger Spekker photometer was employed in these measurements.

** A Hardy color analyzer was used in this work.

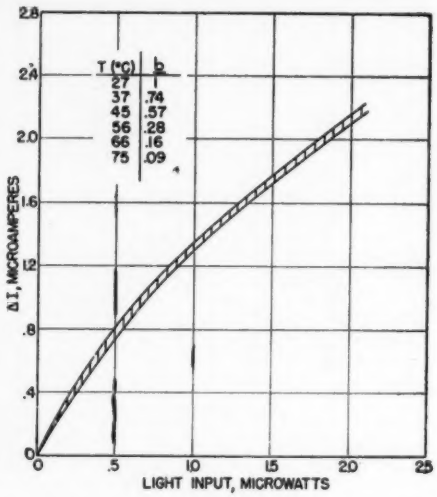

FIG. 15. Conversion of temperature curves into the 27°C characteristic.

0.1 percent and the reflectance 25±1 percent over this spectral range.

From some additional data obtained between 8000 and 12,000A*** on layers of standard thickness, it appears that there is a peak in the transmission curve at about 1.0μ and that about 10 percent of the incident light is transmitted at this wave-length.

Over the entire spectral range investigated the presence of oxygen does not seem to alter materially the shape of the transmission curve.

VIII. RESPONSE TO FLASHES OF SHORT DURATION

In order to determine the build-up and decay characteristics of the photo-current, an investigation was made of cell response to light flashes of extremely short duration.

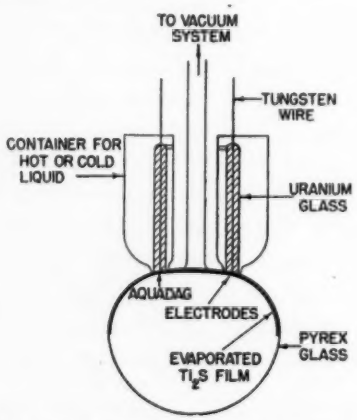

FIG. 16. Cell for thermo-e.m.f. determination.

*** The Gaertner monochromator was employed for this purpose.

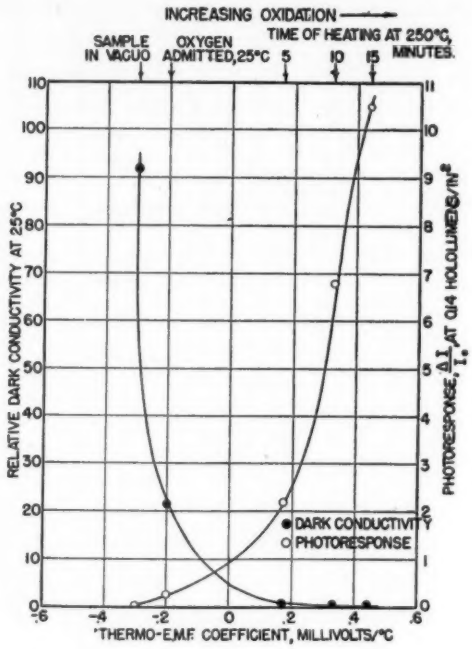

FIG. 17. Relation between dark conductivity, photoresponse, and thermo-e.m.f. coefficient with increasing oxidation.

A. Equipment and Procedure

The incandescent lamp source mounted in front of the monochromator slit was replaced by a discharge tube of the Edgerton type which could be flashed for approximately 3×10^{-6} second by a condenser discharge.

The photo-cell was connected in series with a battery and load resistance in the usual manner. The load resistance was coupled to a cathode follower unit with low input capacitance, approximately 5 $\mu\mu$f, to eliminate frequency distortion, and the cathode follower output was amplified by a single-stage a.c. amplifier.* The output of this amplifier was further amplified by the Y axis amplifier of a DuMont Type 208 oscilloscope, and the trace, which appeared on the screen of a 5LP1 DuMont cathode-ray tube, was photographically recorded. In order to expand the time scale, a multiple sweep arrangement was used which was a modification of the circuit described by Richter.[21]

* The electronic circuits were constructed by M. Haugen.

[21] W. Richter, Electronics **17**, No. 9, 128 (1944).

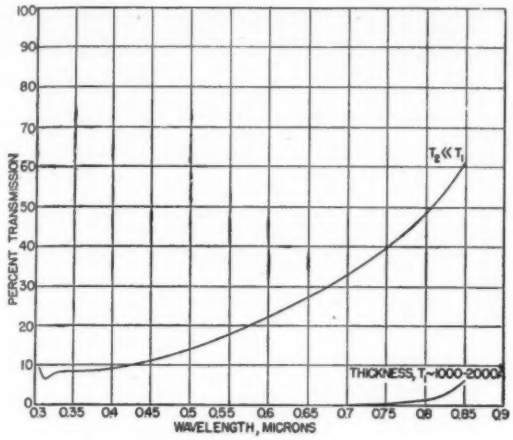

FIG. 18. Transmission of thallous sulfide layers.

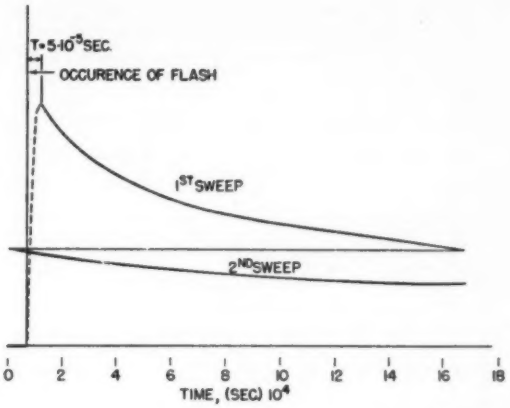

FIG. 19. Oscillograph trace of response to flash.

For our analysis it was desired to determine the change in conductance as a function of time. In order to simplify the interpretation of the various photographed patterns, it was necessary to select load resistance values, R_L, so as to obtain proportionality between output voltage (across R_L), ΔE, and change in cell conductance, ΔG. Since it can be shown that

$$\Delta E = R_L \Delta I = \frac{R_L \Delta G (R_0 - \Delta R) I_0}{G_0 (R_0 - \Delta R + R_L)}, \qquad (7)$$

it is apparent that in order to obtain proportionality between ΔE and ΔG it is necessary that $R_L \ll R_0 - \Delta R$. This condition was fulfilled in the majority of our experiments by employing a load resistance of 10,000 ohms. At extremely low light intensities, however, it was possible to use a load resistance as high as 200,000 ohms.

The flash response of the thallous sulfide photo-cell was studied as a function of voltage, wave-length, light intensity, and temperature. In addition, cells of different resistance and oxidation states were compared under closely similar conditions.

The intensity of the flashes was controlled by altering the slit widths of the monochromator. The intensity of a single flash could not be accurately duplicated, however, since the discharge was not completely reproducible in intensity and location. Nevertheless, a measure of the intensity could be had by determining the peak value of $\Delta G/G_0$ from an examination of the photographed pattern and from the known dark conductance. The relative intensities of the flashes were varied over a range of the order of 3000:1, the lowest intensity being limited only by cell and circuit noise.

For the temperature measurements the electrically heated oven was mounted inside the same shielded container as that enclosing the cathode follower and amplifier circuits. The small capacitance of the cell, about 10 $\mu\mu$f, increased only by about 50 percent in the oven mount.

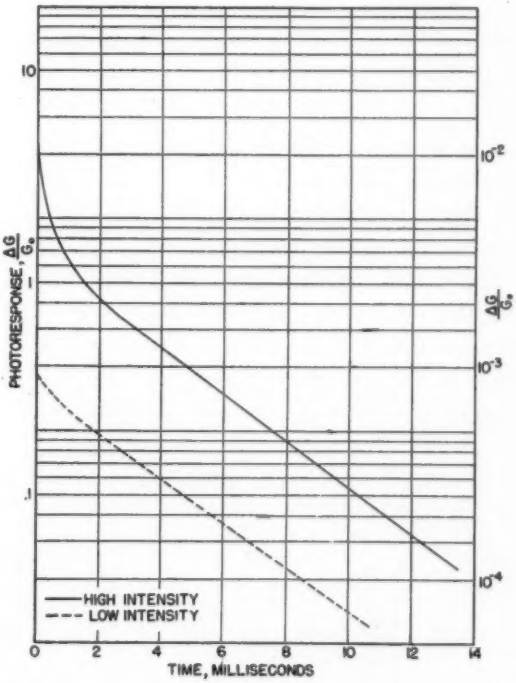

FIG. 20. Decay characteristics for two light intensities.

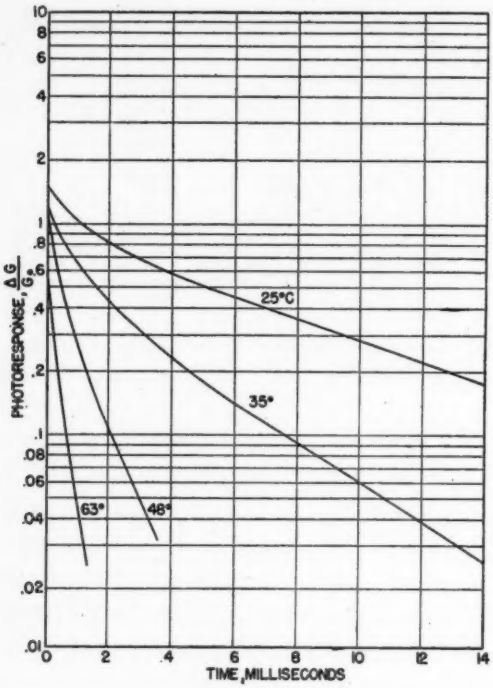

FIG. 21. Decay characteristic as function of temperature.

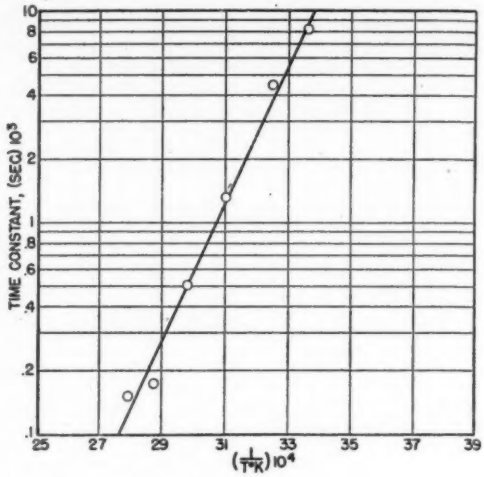

FIG. 22. Temperature dependence of the time constant.

B. Results

All cells thus far investigated exhibit a response characteristic typified by Fig. 19. After the occurrence of the light flash, the photo-current builds up in about 5×10^{-5} second to its maximum value; its decay with time is exponential save for the very beginning of the curve. This can be readily seen in a plot of the photo-response on a logarithmic scale against time (Fig. 20), where the slope is steepest initially and rapidly decreases to a constant value, κ.

The voltage applied to the cell and a change in wave-length of the monochromatic light flash between 0.6 and 1.1μ have no effect upon the shape of the decay characteristic.

Light intensity and temperature, on the other hand, have a pronounced effect. With increasing intensity the initial slope of the log plot becomes progressively steeper while the slope of the linear portion of the curve remains the same (Fig. 20) within the limits of error of about ±10 percent. With increasing temperature, although the time of rise remains unchanged, the cell decay becomes progressively more rapid and the peak in the response curve falls (Fig. 21). The variation of peak response with temperature is a linear function as the data of Table IV show. The time constant, $1/\kappa$, of the exponential portion of the decay curve increases exponentially with the reciprocal of the absolute temperature (Fig. 22). In the one instance where reliable measurements are available, the value of the activation energy (0.65 electron volt) obtained from the slope of this curve is slightly larger than the activation energy, U (0.54 electron volt), determining the dark current dependence on temperature.

TABLE IV. Peak flash response *vs.* temperature.

Peak $\Delta G/G_0$	T°C
1.45	25
1.17	35
1.05	48
0.67	63
0.24	76
0.11	85

On comparing sensitive cells of different resistances and oxidation states (Table V), it appears that the time constant, $1/\kappa$, increases in a very general way with decreasing cell resistance, although no correlation between time constant and composition can be seen. No relationship has been found between the magnitude of the peak in the response curve and $1/\kappa$, R_0, or composition; the data are not included in the table as all measurements were not made at the same intensity level.

On comparing insufficiently oxidized cells at

the same light intensity and applied voltage (Table VI—cell No. 4 of high sensitivity included as a typical end member of the series), it can be seen that the peak yield increases rapidly with oxygen content while the time constant remains relatively unchanged. However, the time constants of cells 59*A* and 5*A* are considerably smaller than Table V would lead one to expect for cells of such low resistance.

TABLE V. Time constant *vs.* dark resistance and composition of sensitive cells.

Cell No.	$(1/\kappa)10^3$, sec.	R_0, megohms*	Composition, mole O_2/mole Tl_2S
114*B*	1.3	840	0.69
2*A*	0.53	450	0.578
18*A*	0.33	322	0.307
60*B*	0.80	225	0.16
166*B*	10.2	140	0.36
138*B*	1	72.5	0.21
4*A*	2.6	51	0.25
6*A*	2.6	26.5	0.339
84*B*	8.7	22.5	0.39
66*B*	4.2	20.4	0.16
40*B*	5.4	15.0	0.39
168*B*	5.2	10.5	0.30
86*B*	11	10.0	0.16
54*B*	21	5.0	0.39
50*B*	28	1.6	0.39
136*B*	56	1.05	0.38
116*B*	37	0.15	0.16

* The differences in values of R_0 from those reported in Table II are the result of long aging.

TABLE VI. Peak yield, time constant, dark resistance *vs.* composition of insensitive cells.

Cell No.	Peak $\Delta G/G_0$	$(1/\kappa)10^3$, sec.	R_0, megohms	Composition, mole O_2/ mole Tl_2S
59*A*	1.5×10^{-5}	1.7	0.018	0
5*A*	3.23×10^{-3}	1.2	0.132	0.119
4*A*	3.79×10^{-1}	2.6	51	0.25

TABLE VII. Frequency response.

Cell No.	$1/\kappa$, sec.*	Frequency, cycles/sec.	30	90	180	360	720
50*B*	3.6×10^{-2}	Signal,** db	104	98	93	86	81
18*A*	3.3×10^{-1}	Signal, db	58	58	58	56	53

* From flash response data.
** Without filter; reference level 0.1μ volt = 0 db.

IX. FREQUENCY RESPONSE

The relative response to modulated light as function of frequency varies widely for different photo-cells as indicated by the data of Table VII. Cells possessing very short time constants, which are not common, exhibit good relative response with frequency over the range investigated. The quantitative relation between frequency response and time constant will be given in connection with a general theoretical discussion to be published in a subsequent paper.

Thallous Sulfide Photo-Conductive Cells

II. Theoretical Discussion*

A. VON HIPPEL AND E. S. RITTNER
Laboratory for Insulation Research, Massachusetts Institute of Technology, Cambridge, Massachusetts

(Received March 4, 1946)

A theory is formulated which is in substantial agreement with all facts reported in a previous paper on thallous sulfide photo-conductive cells. The underlying physical picture is that light is absorbed in the Tl_2S proper and in the presence of oxygen, positive "holes" and negative oxygen ions are formed. The "holes" and ions recombine at a rate proportional to the product of their concentrations. During their lifetime, the negative ions act as space charge compensators for the defect conduction and allow correspondingly higher currents to flow. This space charge compensating action, which is similar to the role played by positive ions in gas discharges, seems to be one essential mechanism of producing secondary photo-effects.

INTRODUCTION

IN a previous paper[1] an account was given of an experimental study of thallous sulfide photo-conductive cells. A satisfactory theory should account for the following facts established by this study:

(1) the dark current and photo-current are proportional to the applied voltage;

(2) the dark conductance decreases exponentially with the reciprocal of the absolute temperature;

(3) the photo-current, which represents a secondary photo-effect, is a non-linear function of the illumination and decreases rapidly with increasing temperature;

(4) the introduction of solute oxygen atoms into the Tl_2S phase reduces the conductivity greatly, changes the material from an excess to a defect conductor, increases the photo-sensitivity many fold, but does not alter materially the transmission of the layer; and

(5) the photo-current produced by a light flash of very short duration builds up to a maximum in about 5×10^{-5} second and decays exponentially with time except initially when the rate of decay is highest and increases with light intensity; the time constant of the exponential portion of the decay characteristic increases exponentially with the reciprocal of the absolute temperature.

I. THE CONDUCTION MECHANISM IN THALLOUS SULFIDE

Crystalline thallous sulfide, according to Ketelaar and Gorter,[2] consists of Tl-S-Tl layers arranged similarly to those in the cadmium iodide (C6) type of structure. The binding between thallium and sulfur atoms cannot be purely ionic as this would require the close juxtaposition of layers of positively charged thallium ions. Moreover, the thallium and sulfur atoms can best be accommodated in the structure by using atomic radii.[2] Similarly, the binding cannot be predominantly metallic because the electronic conductivity of thallous sulfide is too small (10^{-2}–10^{-5} ohm^{-1} cm^{-1} at 25°C) for the metallic bond to contribute appreciably to the cohesion of the crystal. It appears likely, therefore, that the bonding between the sulfur and thallium atoms is covalent (possibly with partial ionic character) and that the attraction between adjacent thallium layers is the result of van der Waals forces similar to the cadmium iodide case. The electrical conductivity is probably restricted to the Tl-Tl planes, in which some of the thallium atoms lie nearly as close together as in thallium metal.

If the electrons or holes needed in the conduction process were not originally present in the compound but were to migrate in from the electrodes, space charge formation would restrict the current density to very small values. This follows from Poisson's equation:

$$\frac{dE}{dx}=\frac{4\pi\rho e}{\epsilon_\infty}, \tag{1}$$

where e=electron charge, E=field strength, ρ=density of charge carriers (is a function only

* This research was carried out under contract OEMsr-1036 with Division 16, Section 16.4 of the National Defense Research Committee and completed in June, 1945. Publication has been delayed because of the war.

[1] A. von Hippel, F. G. Chesley, H. S. Denmark, P. B. Ulin, and E. S. Rittner, J. Chem. Phys. **14**, 355 (1946).

[2] J. A. A. Ketelaar and E. W. Gorter, Zeits. f. Krist. **101**, 367 (1939).

of x), and ϵ_∞ = optical dielectric constant. By replacing ρ by the current density, j,

$$j = \rho e b E = \sigma E, \tag{2}$$

where σ = conductivity and b = mobility; and integrating, the following expression results:

$$E = \left(\frac{8\pi j x}{\epsilon_\infty b} + E_0^2 \right)^{\frac{1}{2}}. \tag{3}$$

Maximum space charge and current density will be attained when the field gradient, E_0, at the electrode from which the charge carriers emigrate ($x=0$) is reduced to zero. By introducing the voltage, V, applied across the sample of length, d,

$$V = \int_0^d E dx; \tag{4}$$

and integrating, the maximum current density possible under space charge conditions is found:

$$j_{\max} = \frac{V^2 b \epsilon_\infty}{d^3} (10^{-15}) \text{ amp./cm}^2. \tag{5}$$

Equation (5) predicts that for a sample of unit length ($d=1$ cm) with 100 volts applied, a mobility of the charge carriers, $b=100$ cm/sec. per volt/cm,[3] and an optical dielectric constant of the order of 10, a current density $j_{\max} \sim 10^{-8}$ amp./cm^2 would be obtained. However, the relation between current density and voltage for Tl_2S is given by Ohm's law (Part I,[1] Section IB, Eq. (1)) rather than by Eq. (5), and a current density of about 1 amp./cm^2 would be observed under the conditions stated.

A more likely assumption is that thermal ionization creates an equilibrium density of electrons and holes in the material:

$$\rho_d = \rho_0 e^{-Q/kT}, \tag{6}$$

where Q = ionization energy and ρ_d = equilibrium density of electrons = equilibrium density of holes. If these charge carriers can traverse the compound with mobilities b_e and b_h without space charge formation, a dark current density, j_d, would result:

$$j_d = \rho_d e E (b_e + b_h). \tag{7}$$

The motion of charge carriers in semiconductors is normally an intermittent process.[4] The electron or hole travels a mean distance $\bar{w}$ in the field direction for an average time, t_f, and is then trapped for a time, t_t. The mobility of the carrier is thus given by

$$b = \bar{w}_0/(t_f + t_t), \tag{8}$$

where $\bar{w}_0 = \bar{w}/E$. The activation energy, u, required to release the trapped carrier is supplied by thermal vibration; hence, t_t will depend on temperature in accordance with Eq. (9):

$$t_t = t_0 e^{u/kT}. \tag{9}$$

For $t_t \gg t_f$, which is usually the case, the mobility may be written

$$b = b_0 e^{-u/kT}. \tag{10}$$

It follows from (6), (7), and (10) that the current density can be expressed as

$$j_d = \rho_0 e E \cdot e^{-Q/kT} (b_{e_0} \exp[-u_e/kT] + b_{h_0} \exp[-u_h/kT]). \tag{11}$$

(Subscripts e and h refer to electrons and holes, respectively.)

It will be recalled that unoxidized Tl_2S (sample No. 2) proved to be an excess conductor and that on oxidation the resistance of the material increased rapidly, while the thermo-voltage changed its sign to indicate defect conductivity (Part I,[1] Section VI, Fig. 17). Consequently, pure thallous sulfide appears to be an "intrinsic" semiconductor in which electrons and holes are mobile, the mobility of the former dominating ($b_e \gg b_h$).

In Part I,[1] Section V, Eq. (4), an empirical relation between conductance, G_0, and temperature had been found:

$$G_0 = a e^{-U/kT}.$$

Also, Table II had indicated that the activation

[3] This value corresponds to the maximum excess electron mobility in the alkali halides (A. Smakula, Goettinger Nachrichten Math. Phys. Kl. 1, 62 (1934)), to the hole mobility in Cu_2O (E. Engelhard, Ann. d. Physik 17, 501 (1933)), and to the order of magnitude of the electron mobility in metals.

[4] A. von Hippel, J. App. Phys. 8, 815 (1937); Phys. Rev. 8, 605 (1940).

energy, U, varied appreciably from cell to cell and that no simple relation existed between U and the state of oxidation. Equation (11) clarifies this situation somewhat. One of the exponential terms involving the mobility normally dominates. In the single exponential function remaining, U is not a simple activation energy but the sum of an ionization energy Q and an activation energy u. It is likely that Q and u will be affected by oxidation. In addition, there is some evidence that in the very thin photo-cell layers a and U are functions of the layer thickness. Moreover, the insulating compound, Tl_2SO_2, formed in the oxidation, will influence U and a in accordance with the amount formed and its location. Therefore, the random variation in U from cell to cell is not surprising.

For the unoxidized material according to (11) the conductivity can be written:

$$\sigma = \rho_0 e b_{e0} \exp\left[(Q+u_e)/kT\right]. \qquad (12)$$

On a thin layer of pure Tl_2S($\sim$500A) values of $\sigma = 10^{-4}$ ohm^{-1} cm^{-1} and of $U = Q + u_e = 0.54$ electron volt were obtained. The magnitude of ρ_0, which corresponds to the number of Tl atoms per cm^3 of thallous sulfide, is 1.1×10^{22}. Hence the maximum mobility of the electrons at room temperature is $b_{e0} = 57$ cm/sec. per volt/cm, in good agreement with values obtained from other systems.[3]

From a consideration of the available space in the Tl_2S structure,* it would appear that the most likely sites for the solute oxygen atoms are in spaces interleaving the Tl-Tl layers. This disposition provides twenty-seven possible locations in the unit cell for accommodating oxygen atoms—the same as the number of sulfur atoms already present. Such strategic location of the oxygens permits them to exert a profound influence on the conductivity. Owing to their large electron affinity, the oxygen atoms serve as electron traps, but the electrons apparently can be released again by thermal agitation. With increasing oxygen content the mobility of the excess electrons must rapidly decrease and the mobility of the holes, while somewhat impaired by lattice distortion, begins to dominate (Part I,[1] Section VI, Fig. 17).

* The advice of F. G. Chesley has been most helpful in these structural considerations.

II. QUALITATIVE DISCUSSION OF THE PHOTO-EFFECT

Two alternative explanations might be offered for the fact that oxygen photo-sensitizes thallous sulfide. A new, photoelectrically active, absorption band may result from the oxidation, or the absorption of the Tl_2S proper may lead to a photoelectric effect when oxygen is present. The transmission measurements (Part I,[1] Section VII) suggest the latter to be the case.

Since the flash response characteristics show that a time of 5×10^{-5} sec. is required for the build-up of the photo-current (Part I,[1] Section VIIIB), it appears that initially an excited state is formed which persists for a short time before giving rise to longer-lived disturbance centers responsible for the secondary photo-effect. The details of this process are probably the following. By the absorption of a light quantum an electron is transferred instantaneously into an excited state. The creation of this state alters the potential field of the neighboring atoms; the nuclei swing into new equilibrium positions, and the lifetime of the excited state is lengthened to about 10^{-5} sec. The electron can then either return to its original state accompanied by realignment of the lattice, or it can be ejected leaving behind a positive hole.

In insulators the latter process would initiate only a primary photo-effect: that is, if electron and hole were to migrate through the material to the electrodes, a maximum photoelectric yield of one electron per ionizing light quantum would be recorded. In semiconductors an additional secondary photo-current should be observed, if the electron and hole do not leave the substance at the same rates.

As is known from gas discharges, one positive ion moving slowly from anode to cathode can allow many fast electrons to pass in the opposite direction because it compensates at any moment the space charge density of the electron current. In the same way a slow hole moving from anode to cathode in pure Tl_2S ($b_e \gg b_h$) would allow b_e/b_h "extra" electrons to flow through the material. Unoxidized thallous sulfide has been found (Part I,[1] Section VIIIB) to exhibit such a photo-response, although the yield obtained is lower than that of the oxidized material by a factor of 10^4 to 10^5.

The presence of an oxygen atom, with its large electron affinity, enormously increases the probability that a photoelectrically excited electron will escape from its parent atom leaving behind a positive hole** and forming a relatively immobile O^- ion. This ion represents the disturbance center producing the secondary photo-effect, and until it recombines with a positive hole, a number of mobile holes can traverse the material. The rate of disappearance of centers is proportional to the total number of O^- ions and also to the total number of positive holes present at any time.

The possibility of effecting conversions from one wave-length to another by means of the a factors in the plots of ΔI *vs.* light intensity (Part I,[1] Section VD) and the lack of dependence of the shape of the decay characteristic on the wave-length of the monochromatic light flash (Part I,[1] Section VIIIB) indicate that the same kind of disturbance center is produced at different wave-lengths.

III. QUANTITATIVE DISCUSSION OF THE PHOTO-EFFECT

A. Response to Steady Illumination

A calculation of the photo-response according to the picture just presented consists of an evaluation of the charge density of electrons and holes prevailing in the material and its change as a function of intensity of illumination.

When thermal equilibrium is established in the dark, the rates of formation, $d\rho_f/dt$, and of recombination, $d\rho_r/dt$, of the charge carriers are equal. Since the recombination rate is proportional to the number of electrons and to the number of holes present at any time, at equilibrium these rates will be proportional to the square of the charge density, ρ_d.

$$\frac{d\rho_f}{dt}=\frac{d\rho_r}{dt}=B\rho_d^2. \tag{13}$$

(B = probability of recombination.)

Under constant illumination a new balance between the rates of recombination and formation is established and the charge density increases from ρ_d to ρ. Hence,

$$B\rho^2=B\rho_d^2+cJ, \tag{14}$$

where c represents the number of charge carrier pairs created per second per unit of volume under an illumination, J, of 1 μwatt/cm^2. The increase in charge carrier density is therefore

$$\Delta\rho=\rho-\rho_d=-\rho_d+\left(\rho_d^2+\frac{c}{B}J\right)^{\frac{1}{2}} \tag{15}$$

and

$$\frac{\Delta\rho}{\rho_d}=-1+\left(1+\frac{cJ}{B\rho_d^2}\right)^{\frac{1}{2}}. \tag{16}$$

Since the photo-current density is given by

$$\Delta j=\Delta\rho eEb_h, \tag{17}$$

while the dark current density is given by

$$j_d=\rho_d eE(b_e+b_h), \tag{18}$$

the ratio of light current to dark current density follows from (16)–(18):

$$\frac{\Delta j}{j_d}=\frac{b_h}{b_e+b_h}\left[-1+\left(1+\frac{cJ}{B\rho_d^2}\right)^{\frac{1}{2}}\right]. \tag{19}$$

In the sensitive, oxidized cell where $b_e \ll b_h$, (19) reduces to

$$\frac{\Delta j}{j_d}=-1+\left(1+\frac{cJ}{B\rho_d^2}\right)^{\frac{1}{2}}. \tag{20}$$

Values of $\Delta j/j_d$ calculated from (20) for a sensitive cell agree within experimental error with measured values of $\Delta I/I_0$, as can be seen in Table I.

TABLE I. Agreement between measured and calculated response to continuous illumination.

Source	Illumination μ watts/cm^2	$\Delta I/I_0$ observed	$\Delta j/j_d$ calculated	
White light	9.35	2.33	2.30	
	23.0	3.94	4.02	
	42.1	5.85	5.72	
	84.5	9.0	8.46	$\frac{c}{B\rho_d^2}=1.05$
	214	14.3	14.1	
	758	24.6	27.2	
$\lambda=0.9\mu$	0.0877	0.176	.165	
	0.175	0.33	.315	
	0.263	0.45	.440	
	0.351	0.55	.560	$\frac{c}{B\rho_d^2}=4.07$*
	0.438	0.64	.670	
	0.527	0.71	.778	

** The positive holes can probably be identified with Tl^+ ions located at lattice points.

* The value of $c/B\rho_d^2$ at any other wave-length for this cell is given by (4.07) $\times$ (a factor). (Part I (reference 1), Section VD.)

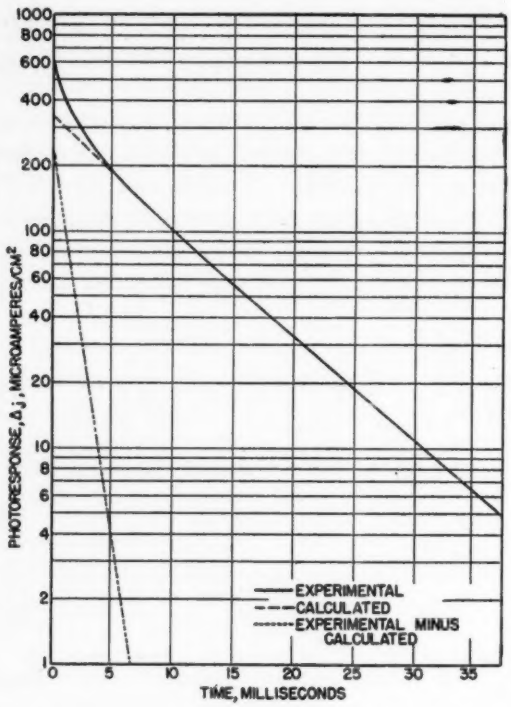

FIG. 1. Experimental and calculated decay characteristics (j_d = microamperes/cm²).

For incompletely oxidized cells (19) fits the data better than (20) because the excess conductivity is still appreciable.

B. Response to Flash Illumination

Under flash illumination the rise of the current occurs as soon as the charge carrier pairs are created. The number of these charge carriers should be proportional to the number of quanta absorbed. If the rate of formation of the pairs is much faster than the rate of their recombination, the peak of the current transient should be proportional to the light intensity.

The decay characteristic can be calculated from the differential equation expressing the rate of disappearance of charge

$$d\rho/dt = B(\rho_d^2 - \rho^2). \tag{21}$$

Introducing $\Delta\rho$, the increase in charge carrier density above ρ_d,

$$d\Delta\rho/dt = -B\Delta\rho(\Delta\rho + 2\rho_d), \tag{22}$$

rewriting (22)

$$d\Delta\rho\left(\frac{1}{\Delta\rho} - \frac{1}{\Delta\rho + 2\rho_d}\right) = -2\rho_d B dt, \tag{23}$$

and integrating (23)

$$\frac{\Delta\rho}{2\rho_d + \Delta\rho} = \frac{\Delta\rho_p}{2\rho_d + \Delta\rho_p} \exp(-2\rho_d B t) \tag{24}$$

($\Delta\rho_p$ = maximum charge carrier pair density produced by the light flash at $t=0$ which corresponds to about 5×10^{-5} sec. after occurrence of the flash), the equation for $\Delta\rho$ is obtained:

$$\Delta\rho = \frac{\Delta\rho_p{}^2\rho_d \exp(-2\rho_d B t)}{2\rho_d + \Delta\rho_p(1 - \exp(-2\rho_d B t))} = \frac{\Delta\rho_p \exp(-2\rho_d B t)}{1 + \frac{\Delta\rho_p}{2\rho_d}(1 - \exp(-2\rho_d B t))}. \tag{25}$$

The photo-current density, Δj, plotted logarithmically as function of time, should therefore follow the law

$$\ln \Delta j = \ln \Delta j_p - 2\rho_d B t - \ln\left[1 + \frac{\Delta\rho_p}{2\rho_d}(1 - \exp(-2\rho_d B t))\right], \tag{26}$$

where $\Delta j_p = \Delta\rho_p e E b_h$.

Differentiating (26), the slope is found to be $-(2\rho_d + \Delta\rho_p)B$ at $t=0$ and $-2\rho_d B$ at $t=\infty$. Hence, the final slope of the decay curve is independent of light intensity while the magnitude of the initial slope increases with the illumination level, in qualitative agreement with the experimental data (Part I,[1] Section VIIIB, Fig. 20).

The constants needed to calculate the decay characteristic from (26) can be obtained in the following way. The quantity $2\rho_d B$ is equal to the final slope of the curve, and the extrapolation of this straight line to $t=0$ gives an intercept

$$\alpha = \frac{\Delta\rho_p}{2\rho_d} 2j_d \Big/ \left(1 + \frac{\Delta\rho_p}{2\rho_d}\right), \tag{27}$$

from which $\Delta\rho_p/2\rho_d$ can be computed. Substituting the known value, Δj_1, at $t_1 (t_1 \gg 1/2\rho_d B)$ in (26), the initial intercept, Δj_p, is obtained.

Agreement between experimental decay characteristics and those calculated from (26) is not very good at the initial portion of the curves (Fig. 1). The difference between experimental

and theoretical characteristics is shown by the dotted curve in the figure, the height and shape of which suggest that an appreciable fraction, $[\Delta\rho_p'/(\Delta\rho_p+\Delta\rho_p')]$, of the total number of disturbance centers decay at a faster rate than that predicted by (26).

This situation may be accounted for by the following hypothesis. When the oxygen content of the solid solution is high, the electron affinity of an oxygen atom will be lowered by the presence of a close oxygen neighbor and the probability of recombination of the corresponding O^- ion with a Tl^+ hole will be increased to B'. In general, the number of oxygen close neighbors surrounding an oxygen atom will vary statistically from zero to six and a similar statistical distribution of time constants is to be expected. It is the longest of these time constants, however, that exerts by far the profoundest effect on the response to steady illumination.

C. Lifetime of the Photoelectric Centers

On the basis of the preceding discussion, the average lifetime, τ, of the disturbance centers can now be calculated.

If an initial charge density, $\Delta\rho_p$, is created by a light flash, τ is defined by the equation

$$\tau=\int_0^\infty \frac{\Delta\rho dt}{\Delta\rho_p}, \tag{28}$$

or according to (25)

$$\tau=\int_0^\infty \frac{2\rho_d \exp(-2\rho_d Bt)dt}{2\rho_d+\Delta\rho_p(1-\exp(-2\rho_d Bt))}. \tag{29}$$

By introducing $x=\exp(-2\rho_d Bt)$ and

$$dx=-2\rho_d B \exp(-2\rho_d Bt)dt,$$

Eq. (29) can be rewritten

$$\begin{aligned}\tau&=\frac{1}{B}\int_0^1 \frac{dx}{2\rho_d+\Delta\rho_p(1-x)}\\&=-\frac{1}{B\Delta\rho_p}[\ln\{2\rho_d+\Delta\rho_p(1-x)\}]_0^1\\&=\frac{1}{B\Delta\rho_p}\ln\left(1+\frac{\Delta\rho_p}{2\rho_d}\right).\end{aligned} \tag{30}$$

The average lifetime, therefore, decreases with increasing light intensity. For very small light intensities $(\Delta\rho_p \ll 2\rho_d)\tau$ becomes

$$\tau=\frac{1}{2\rho_d B}=\frac{1}{\kappa} \tag{31}$$

(for definition of κ see Part I,[1] Section VIIIB).

D. Frequency Response

Runge and Sewig[5] have proposed a theory to account for the photo-effect in thallous sulfide photo-conductive cells based on the assumption that light creates disturbance centers which decay exponentially with time. This theory is inadequate to explain most of the data obtained in our work.[1] However, their assumption is valid at very low intensity levels, as is shown by flash response results (Part I,[1] Section VIIIB, Fig. 20). Hence, the equation derived by these authors for the photo-current produced by a square-wave modulated light signal can be employed to calculate the frequency response of the cell at the low intensity levels employed in the standard test set.[6,7] In this equipment the d.c. component and all harmonics of the photo-current above the fundamental frequency are eliminated by the amplifier system. Therefore, the relationship between the instantaneous photo-current, Δi, and the time, t; the frequency, $\omega/2\pi$; the d.c. current, Δi_p, produced by steady illumination of the peak value; and the time constant, $1/\kappa$, is given by

$$\Delta i=\frac{2\kappa\Delta i_p}{\pi}\left(\frac{\omega}{\omega^2+\kappa^2}\sin\omega t+\frac{\kappa}{\omega^2+\kappa^2}\cos\omega t\right) \tag{32}$$

or

$$\Delta i=\frac{2\kappa\Delta i_p}{\pi(\omega^2+\kappa^2)^{\frac{1}{2}}}\sin(\omega t+\theta), \tag{33}$$

where $\tan\theta=\kappa/\omega$. The peak amplitude, A, of the current is thus given by

$$A=2\kappa\Delta i_p/\pi(\omega^2+\kappa^2)^{\frac{1}{2}}, \tag{34}$$

or the r.m.s. voltage, S, developed across the

[5] I. Runge and R. Sewig, Zeits. f. Physik 62, 726 (1930).
[6] W. L. Hole, N.D.R.C. Report No. 16.4—Special No. 9 (1944).
[7] L. N. Holland, N.D.R.C. Report No. 16.4—Special No. 6 (1944).

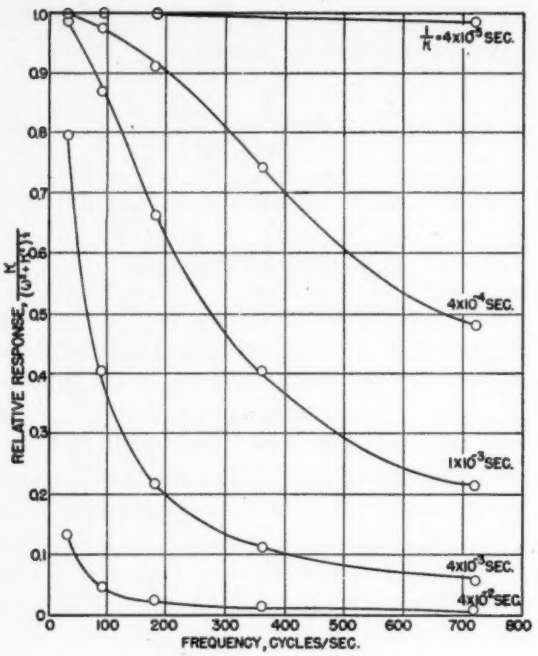

FIG. 2. Relative response *vs.* frequency for different values of the time constant.

load resistor, R_L, of the input circuit amounts to

$$S=\frac{2\kappa\Delta i_p R_L}{\pi(\omega^2+\kappa^2)^{\frac{1}{2}}(2)^{\frac{1}{2}}}. \tag{35}$$

The quantity $\kappa/(\omega^2+\kappa^2)^{\frac{1}{2}}$, representing the relative response with frequency, has been plotted in Fig. 2 as function of the modulating frequency for different values of the time constant, $1/\kappa$. For cells which decay quite slowly ($\kappa^2 \ll \omega^2$) the relative response is inversely proportional to the frequency and independent of κ; while when κ becomes of the same order as ω, the shape of the response characteristic is highly dependent upon the magnitude of the time constant.

It follows from (35) that the frequency response of a cell can be calculated if κ is determined from flash response data and if the photocurrent, Δi_p, resulting from the exposure to an unmodulated signal flux of one microhololumen is measured.* Tables II and III show that satisfactory agreement between calculated and measured values of S is obtained.

* Δi_p can also be calculated from Eq. (27) of Part I (reference 1) using the value of $c/B\rho_d^2$ obtained from measurements at higher levels of illumination and correcting for the fact that only a fraction of the cell surface is illuminated in the test set.

It is of interest to consider the change in cell response resulting from a change in the time constant, $1/\kappa$, keeping all other factors constant. Since Δi_p is proportional to the average lifetime of the disturbance centers and hence proportional to $1/\kappa$ at low levels of illumination, $(\omega^2+\kappa^2)^{-\frac{1}{2}}$ should be representative of the peak amplitude, A. Values of $(\omega^2+\kappa^2)^{-\frac{1}{2}}$ for various values of $1/\kappa$ and for $\omega/2\pi=90$ cycles are shown in Table IV. The output at 90 cycles increases with time constant; however, there is little to be gained in increasing $1/\kappa$ beyond the values of the time constants of the majority of cells made by present methods. Improvement of the frequency response, which requires a reduction in the time constant, can be obtained only at the expense of the absolute signal level.

Since $\kappa=2\rho_d B$, any means which can be utilized to increase ρ_d (or the apparent ρ_d) can be employed in reducing the time constant. Such means include exposure of the cell to high temperatures or to background unmodulated illumination.

E. Photoelectric Yield

The space charge compensating action of the disturbance centers during their average life-

TABLE II. Comparison of calculated and measured signal voltages at 90 cycles.

Cell No.	$1/\kappa$, sec.	Δi_p, μ amp.	R_L, megohms	Signal, db (reference level 0.1μ volt =0 db) Calculated	Measured
50*B*	3.6×10^{-2}	0.20	2.5	101	98
54*B*	2.1×10^{-2}	0.07	10	108	108
84*B*	8.7×10^{-3}	0.02	40	117	115
40*B*	5.2×10^{-3}	0.025	20	117	114
66*B*	4.2×10^{-3}	0.015	40	111	110
18*A*	3.3×10^{-4}	**	0.5	—	58

** Δi_p too small to measure; calculated value from measured signal $=3.6\times10^{-4}$ μamp.

TABLE III. Comparison of calculated and measured frequency response.

Cell No.	Frequency, cycles/sec.	30	90	180	360	720
50*B*	*S*, db calculated	107	101	95	89	83
	measured	104	98	93	86	81
54*B*	*S*, db calculated	114	108	102	96	90
	measured	112	108	103	94	88
18*A*	*S*, db calculated*	58	58	57.5	56	53
	measured	58	58	58	56	53

* Calculations made relative to measured response at 90 cycles.

time, τ, allows z holes to traverse the length, d, of the semiconductor where

$$z=\tau b_h E/d. \tag{36}$$

If the fraction of the incident radiation absorbed by the layer is f, and if the photoelectrically excited electrons escape from their parent atoms with a probability, P, the quantum yield is given by

$$\eta=fP\tau b_h E/d. \tag{37}$$

The photoelectric yield is a function of temperature for several reasons. As is shown by the data of Table IV, Part I,[1] the variation of the peak of the flash response curve with temperature can be expressed by an equation of the form

$$\Delta G_p/G_0=p-qT, \tag{38}$$

where $p=2.0$ and $q=.0222$ for T in °C and for the particular cell measured; or

$$\Delta G_p=pG_0-qG_0T$$
$$=pae^{-U/kT}-qTae^{-U/kT}. \tag{39}$$

(See (4), Part I.[1]) Hence, ΔG_p increases at first and later decreases with temperature, becoming zero at 90°C. Since ΔG_p is proportional to fP, this product also varies with temperature in accordance with (39).

The density of charge carriers, ρ_d, increases rapidly with temperature according to (6); therefore, if B is constant, the time constant for low light intensities should increase exponentially with the reciprocal of the absolute temperature. This has been experimentally verified (Part I,[1] Fig. 22); however, the slope of the plot of $\log 1/\kappa$ *vs.* $1/T$ was steeper than the corresponding plot of $\log G_0$ *vs.* $1/T$. This suggests that B is not a constant but varies with temperature in the following way:

$$B=B_0e^{-s/kT}. \tag{40}$$

Finally, b_h should increase somewhat with temperature (10), but the activation energy, u_h, is so small (see IIIF) that this effect is of minor importance.

The b factors (Part I,[1] Fig. 15) representing the over-all yield as a function of temperature are defined by the relation

$$b=\eta_{T°K}/\eta_{300°K} \quad \text{(for } \lambda=\text{constant)}$$
$$=f_{T°K}P_{T°K}\tau_{T°K}/f_{300°K}P_{300°K}\tau_{300°K}. \tag{41}$$

TABLE IV. Dependence of $(\omega^2+\kappa^2)^{-\frac{1}{2}}$ on $1/\kappa$ at 90 cycles.

$(\omega^2+\kappa^2)^{-\frac{1}{2}}$	$1/\kappa$, sec.
4×10^{-5}	4×10^{-5}
3.9×10^{-4}	4×10^{-4}
8.7×10^{-3}	1×10^{-3}
1.6×10^{-3}	4×10^{-3}
1.76×10^{-3}	4×10^{-2}
1.767×10^{-3}	∞

F. Calculation of Fundamental Constants

If the value of one constant is assumed, it is possible to calculate the values of the other fundamental constants from experimental measurements. This has been done for the sensitive cell No. 84*B*.

The hole mobility, b_h, can be obtained from (37) using measured values of quantum yield ($\eta=1.8$ electrons/quantum at $\lambda=0.6\mu$ and $E=124$ volts/cm), time constant at low levels of illumination ($\tau=9.13\times10^{-3}$ second, from final slope of Fig. 1), distance between alternate grids ($d=0.19$ cm), fraction of the incident radiation absorbed by the layer ($f=0.75$ at 0.6μ from absorption measurements), and assuming the probability that a photoelectrically excited electron will escape from its parent atom, P, to be about 0.4:

$$b_h=0.96\frac{\text{cm}}{\text{sec.}}\Big/\frac{\text{volt}}{\text{cm}}.$$

The maximum charge carrier pair density, $\Delta\rho_p$, produced by a single light flash (of unknown absolute intensity) can be computed from the calculated initial intercept of the flash response curve ($\Delta j_p=347\times10^{-6}$ amp./cm² at $\lambda=0.9\mu$ and $E=215$ volts/cm), the calculated value of b_h, and (26).

$$\Delta\rho_p=1.0\times10^{13}\text{ cm}^{-3}.$$

The extrapolation of the straight line portion of the flash curve yields a value of $\Delta\rho_p/2\rho_d=0.22$. Hence,

$$\rho_d=2.4\times10^{13}\text{ cm}^{-3}.$$

Since the final slope, $2\rho_dB$, is 109.5 sec.$^{-1}$, the recombination probability, B, is

$$B=2.3\times10^{-12}\text{ cm}^3\text{ sec.}^{-1}.$$

Similarly, the average probability of recombination, B', of the faster decaying centers is about

$$B'\sim1.6\times10^{-11}\text{ cm}^3\text{ sec.}^{-1},$$

and these centers comprise about 43 percent of the total number. (See initial intercepts of Fig. 1.)

From the calculated value of ρ_d, the known values of ρ_0 (1.1×10^{22}) and T (300°K), and (6), the thermal ionization energy can be calculated.

$$Q=0.51 \text{ electron volt.}$$

This value agrees with the measured thermal activation energy, U, within experimental error. Hence,

$$u_h=U-Q=0.$$

The quantum yield measured under steady illumination yields a value of $c/B\rho_d^2=11.0$, which together with the values of B and ρ_d gives the number of charge carrier pairs created per second per unit of volume under an illumination of 1 μwatt/cm^2 ($\lambda=0.6\mu$).

$$c=1.4\times10^{16} \text{ cm}^{-3} \text{ sec.}^{-1} \mu\text{watt}^{-1} \text{ cm}^2.$$

This corresponds to an equilibrium charge density created by this illumination of $\Delta\rho=5.9\times10^{13}$ cm^{-3}.

The constant, c, can also be calculated directly from the number of effective quanta absorbed in the photo-sensitive layer of thickness δ ($\delta=5\times10^{-5}$ cm).

$$c=\frac{5.03\times10^{12}\lambda_\mu fP}{\delta}$$

$$=1.8\times10^{16} \text{ cm}^{-3} \text{ sec.}^{-1} \mu\text{watt}^{-1} \text{ cm}^2. \quad (42)$$

In view of the uncertainty in the magnitude of P, this result is in good agreement with the previous calculation.

Finally, the capture cross section, A, of an oxygen ion defined by

$$A=B/v \quad (43)$$

can be obtained if an estimate is made of the "instantaneous" velocity, v, of a thallium hole. The maximum frequency with which a Tl^+ hole can be exchanged from thallium to thallium neighbor by thermal vibration can be calculated to a first approximation from the Debye temperature of thallium metal:

$$\nu_{\max}=k\theta/h$$
$$=2.1\times10^{12} \text{ sec.}^{-1}. \quad (44)$$

where k = Boltzmann constant, h = Planck constant, and θ = Debye temperature = 100°K. Multiplying $\nu_{\max}$ by the average thallium − thallium distance in Tl_2S (4×10^{-8} cm), the maximum velocity, $v_{\max}$, of a thallium hole is found to be

$$v_{\max}=8.4\times10^4 \text{ cm sec.}^{-1}$$
$$=v \text{ for } u_h=0$$

yielding a capture cross section of

$$A=2.74\times10^{-17} \text{ cm}^2,$$

an area which is unreasonably small. This indicates that many thallium holes collide with oxygen ions without recombining. Evidence has already been cited to support this supposition (see (40)), an activation energy, $s=0.11$ electron volt, having been measured on a different cell (Part I,[1] Section VIIIB). If this value of s also applies to cell No. 84B, the maximum probability of recombination is

$$B_0=1.61\times10^{-10} \text{ cm}^3 \text{ sec.}^{-1},$$

leading to a value of

$$A=19.1\times10^{-16} \text{ cm}^2,$$

which corresponds to a circular cross section of radius 2.46A. This is a reasonable order of magnitude as the distance from center to center of a Tl^+ ion and O^- ion in contact is about 2.5A.

ACKNOWLEDGMENT

Shortly before this work was completed, Dr. Uhlenbeck informed us about the theoretical treatment of the thallous sulfide cell and the measurements carried out at the University of Michigan, which were submitted to Division 16.4 of N.D.R.C. as "Special Report 26" by A. W. Ewald, W. L. Hole, and G. E. Uhlenbeck. The calculations of these authors have been based on the model of an excess semiconductor with impurity centers, as used by Mott and Gurney.[8] This mathematical treatment can be adapted with slight modification to the discussion of thallous sulfide as an "intrinsic" semiconductor, and we have profited from it for our discussion of response to continuous and to flash illumination.

[8] N. F. Mott and R. W. Gurney, *Electronic Processes in Ionic Crystals* (Oxford University Press, New York, 1940), p. 191.

Notes on the Infra-Red Spectrum and Molecular Structure of Ozone

ARTHUR ADEL AND DAVID M. DENNISON
University of Michigan, Ann Arbor, Michigan
(Received March 22, 1946)

The nature of the fine structure of the band at 14.2μ in the absorption spectrum of ozone has been determined with prism and grating spectrometers. These data, together with the fine structure of the 9.57μ band (previously resolved in the solar spectrum) render possible an unambiguous choice between the divergent views currently held with regard to the structure of the ozone molecule. It is concluded that the form of the isoceles triangle is acute, with the apex angle in the neighborhood of 34°.

I. INTRODUCTION

NUMEROUS attempts have been made to analyze the infra-red spectrum and determine the molecular structure of ozone.

Prior to the definitive (although low dispersion) experiments of Hettner, Pohlman, and Schumacher[1] in 1934, these attempts were unsuccessful, mainly because

(1) they were made in ignorance of the existence of the ozone band at 14.2μ, and
(2) they mistakenly identified as due to ozone the intense bands of nitrogen-pentoxide (N_2O_5), a contamination difficult to avoid in the preparation of ozone.

Since 1934 the attempts at solving the ozone problem have been inconclusive because of the persisting lack of accurate information regarding the band envelopes and fine structures.

The history of the problem prior to the work of Hettner, Pohlman, and Schumacher[1] is given by Gerhard,[2] and since that time by Simpson.[3] It is sufficient for our present purpose to point out that Hettner, Pohlman, and Schumacher[1] assumed a Q-branch for the 9.57μ band. The envelopes of the bands at 4.75μ and 14.2μ were plainly Q-branch and doublet, respectively. On the assumptions of central forces and the frequency assignment $\nu_1(4.75\mu)$, $\nu_2(9.57\mu)$, $\nu_3(14.2\mu)$ this led to an apical angle of 39 degrees.

Low dispersion solar spectra show, however, an apparently doublet envelope for the band at 9.57μ. Adel, Slipher, and Fouts[4] showed that, using this identification, imaginary values for the apical angle are obtained on either central or valence forces, provided the bands at 4.75μ, 9.57μ, and 14.2μ are still regarded as fundamentals.

Continuing the assumption of doublet structure for the 9.57μ band (which we believe to be a mistaken one), but substituting the weak band at 5.75μ for the strong one at 4.75μ, and giving preference to a valence force field, Penney and Sutherland[5] were led by the frequency assignment $\nu_1(9.57\mu)$, $\nu_2(14.2\mu)$, $\nu_3(5.75\mu)$ to an apical angle of 164 degrees.

In a critical discussion of the electronic structure of the ozone molecule Mulliken[6] favors the acute angle form of the molecule designated by Hettner, Pohlman, and Schumacher.[1] But recently Shand and Spurr[7] have concluded from electron diffraction experiments that the apical angle of the ozone molecule must be obtuse, 127 ± 3 degrees.

The correctness of this last result was assumed by Miss D. M. Simpson.[3] Continuing the tradition of the doublet envelope for 9.57μ she finds the most probable assignment of frequencies to be $\nu_1(5.75\mu)$, $\nu_2(9.57\mu)$, $\nu_3(4.75\mu)$.

In deciding between an acute and an obtuse form for the ozone molecule, the envelope form of the 9.57μ band is crucial. And since, in all analytical attempts to date, this form is at least somewhat uncertain, it is desirable to obtain

[1] G. Hettner, R. Pohlman, and H. J. Schumacher, Zeits. f. Physik **91**, 372 (1934).
[2] S. L. Gerhard, Phys. Rev. **42**, 622 (1932).
[3] D. M. Simpson, Trans. Faraday Soc. **41**, 209 (1945).
[4] A. Adel, V. M. Slipher, and O. Fouts, Phys. Rev. **49**, 288 (1936).
[5] W. G. Penney and G. B. B. M. Sutherland, Proc. Roy. Soc. **A156**, 654, 678 (1936).
[6] R. S. Mulliken, Rev. Mod. Phys. **14**, 204 (1942).
[7] W. Shand and R. A. Spurr, J. Am. Chem. Soc. **65**, 179 (1943).

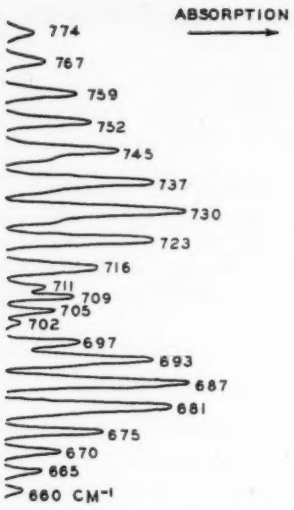

FIG. 1. Ozone 14.1 mμ.

new and independent evidence. This has been achieved by comparing the fine structure of the doublet band at 14.2μ with the fine structure of the band at 9.57μ.

The fine structure of 9.57μ is already at hand in the infra-red solar spectrum.[8] It remained to resolve the band at 14.2μ.

II. EXPERIMENTAL

Ozone was prepared according to the method of Goldstein,[9] and the 14.2μ band was examined both with a NaCl prism and a 2400-line grating. The prism curve, Fig. 1, is remarkably suggestive of the perpendicular band of a symmetrical top molecule.* Asymmetry in the lines of Fig. 1 suggests a complex line structure, and this is confirmed by the grating analysis, Fig. 2.

The structures of the bands at 9.57μ and 14.2μ are fundamentally dissimilar. And since 14.2μ is a near-perpendicular band, 9.57μ must be a near-parallel band (Q-branch).

As a further aid in discussing the ozone spectrum the envelopes of the bands at 3.28μ and 3.57μ have been re-examined, Fig. 3.

III. DISCUSSION

The first and the most crucial point in the interpretation of the infra-red spectrum of ozone is the identification of the fundamental bands. The investigation of Hettner, Pohlman, and Schumacher[1] showed that the most intense regions of absorption are those at 4.75, 9.57, and 14.2μ. From 16 to 27μ (the limit of their observations) ozone is almost completely transparent and it is unlikely that any fundamental bands would lie beyond 27μ. It is therefore natural to identify the three regions just mentioned with the three fundamental frequencies of the molecule. An alternate scheme which has been considered by some investigators would be to take the band at 9.57μ as a fundamental but to identify the 4.75μ region as its first overtone. The second overtone must then be assigned to the weak band at 3.28μ. The difficulty with this scheme is that the three frequencies, namely, 1043, 2108, and 3050 cm^{-1} cannot be placed in a series of the type demanded by the theory of anharmonic oscillators. This is immediately evident since 2108 is greater than twice 1043, while 3050 is less than three times 1043.

For these reasons it seems very probable that the three fundamental frequencies of ozone are $\nu_1=2108$, $\nu_2=1043$, and $\nu_3=705$ cm^{-1}, corresponding to the three most intense regions of absorption.

The second crucial point is concerned with the fine structure of the bands. The new experimental evidence reported in this paper sheds a revealing light upon the problem. The long wavelength band at 14.2μ is found to have a structure consisting of widely spaced lines, each of which is multiple. The average value of the coarse spacing is about 5.7 cm^{-1} and is fairly regular although there is a rather large convergence. The magnitude of the coarse spacing indicates

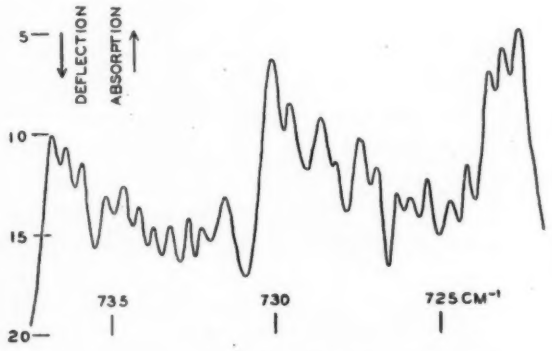

FIG. 2. Ozone 13.7 mμ.

[8] A. Adel, Astrophys. J. 94, 451 (1941).
[9] E. Goldstein, Ber. d. d. Chem. Ges. 36, 3042 (1903).
* We are indebted to Mr. E. A. Boettner of the Wyandotte Chemicals Corporation for the use of their prism spectrometer in obtaining the data for this curve.

unequivocally that the electric moment corresponding to this frequency must oscillate along the middle axis of inertia. (The oscillating electric moment of a triatomic molecule can only be directed along either the least or the middle axis of inertia. When it is directed along the middle axis, the rotational selection rules predict a widely spaced series of lines characteristic of the rapid rotations about the least axis of inertia. When the electric moment oscillates along the least axis of inertia, these transitions are forbidden.)

The band at 9.57μ has been examined by Adel[8] in the solar spectrum. Its structure was found to consist of fairly regularly spaced lines with an average spacing constant of around 1 cm^{-1}. Gerhard's[2] measurements on the 4.75μ band likewise reveal a very narrow spacing which is also of the order of 1 cm^{-1}. Thus for both of these bands the electric moment must oscillate along the least axis of inertia.

These facts admit of only one interpretation. The apical angle of the ozone molecule must be less than 60 degrees. This conclusion is the result of broad and general considerations. A further examination serves to confirm it in detail and leads to the following points.

1. The spacing of the fine structure lines in a band where the electric moment oscillates along the least axis of inertia is of the order of $\Delta\nu = (h/8\pi^2c)(1/I_A+1/I_B)$. (Of course this molecule is an asymmetric rotator and the spacing of the fine structure lines must be irregular. However, when two of the moments of inertia, in this case the greatest and middle moments, are approximately equal, the above formula gives a rough representation of the fine structure.) Setting in the observed spacing of 1 cm^{-1}, one obtains $2I_AI_B/(I_A+I_B)\cong 56\times10^{-40}$ g cm^2.

The spacing of the fine structure lines in a band with changing electric moment along the middle axis of inertia is of the order of $\Delta\nu=(h/8\pi^2c)(2/I_C-1/I_A-1/I_B)$. This approximation is subject to the same limitations as those governing the spacing in the other type of band. In the ozone molecule, the identity of the oxygen nuclei and the fact that their nuclear spin is zero means that every other line will be missing and the observed spacing will have twice the value given above. Setting in the experimental

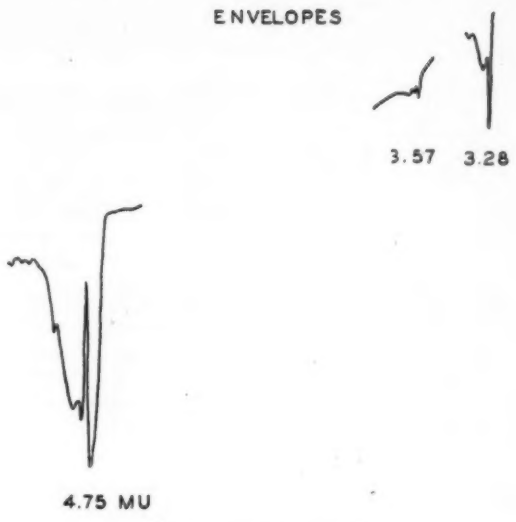

FIG. 3. Ozone envelopes.

value for $\Delta\nu$, combining with the earlier result, and remembering that for a plane molecule $I_A=I_B+I_C$, one obtains $I_A\cong 64\times10^{-40}$, $I_B\cong 50\times10^{-40}$, and $I_C\cong 14\times10^{-40}$ g cm^2. The corresponding apical angle is 34 degrees. It must be emphasized that these numerical results are extremely rough both from the experimental and the theoretical sides. Our estimate of their order of accuracy is ± 20 percent. In order to obtain the moments of inertia more exactly the most promising procedure appears to be to resolve the complete fine structure of the 14.2μ band with a grating spectrometer. The lines can then be correlated with the energy levels of an asymmetric rotator and the moments of inertia determined. We hope to make this investigation in the near future.

2. If the molecule of ozone has the form of an isosceles triangle with an apical angle of less than 60 degrees, it is quite probable that the forces can be satisfactorily approximated by central forces rather than by valence forces. A calculation of the force constants yields results which are substantially in agreement with those obtained by Hettner, Pohlman, and Schumacher. The apical angle turns out to be 39 degrees, the force constant between the oxygens forming the base of the triangle, $K=34\times10^5$ dynes/cm and the constant between the apical and one of the base oxygens, $K'=6.2\times10^5$.

3. The weaker bands of ozone may be expressed as overtones and harmonics of the three fundamentals. These have been assembled in

TABLE I.

Identification	Calc. frequency	Obs. frequency	Obs. type
ν_3	——D	705	Doublet
ν_2	——Z	1043	Zero branch[a]
$\nu_2+\nu_3$	1748D	1740	Doublet[b]
ν_1	——Z	2108	Zero branch[c]
$\nu_1+\nu_3$	2813D	2800	Zero branch?[d]
$\nu_1+\nu_2$	3151Z	3050	Zero branch?[d]

[a] This band has often been thought to be of the doublet type. A study of Adel's curve shows an intense region of absorption at 1041 cm^{-1} which is undoubtedly a zero branch displaced through convergence.
[b] While the resolution is not great, the curve of Hettner, Pohlman, and Schumacher distinctly favors a doublet structure for this band.
[c] Gerhard's work, as well as ours, shows that this is clearly a zero-branch band.
[d] Figure 3 shows envelopes which more nearly resemble zero branches than doublets. The evidence is inconclusive for both of these overtone bands however.

Table I. The first column gives the designation of the band and the second the calculated frequency and the predicted type (D=doublet band, Z=zero-branch band). The third column lists the observed frequency while the fourth describes its type.

IV. CONCLUSION

The present interpretation of the ozone spectrum is both simple and direct and is, in almost all respects, self-consistent. The three most intense regions of absorption are identified with the three fundamental frequencies. The weaker regions are assigned to those overtone combinations which are normally the most intense, namely, $\nu_2+\nu_3$, $\nu_1+\nu_3$ and $\nu_1+\nu_2$. The calculated frequencies of the overtones are, in each case, slightly larger than the observed frequencies. This again is the usual situation.

The fine structure of the bands leads to an apical angle of 34 degrees which is in good agreement with the apical angle of 39 degrees calculated independently from the positions of the fundamental bands.

The dimensions of the molecule as roughly estimated from the fine structure are reasonable. The distance between the oxygens forming the base of the isosceles triangle is 1.0×10^{-8} cm whereas the distance between the atoms in O_2 is 1.208×10^{-8}. The envelopes of the bands—a distinct doublet for ν_3 and zero-branch bands for ν_1 and ν_2—are in agreement with the predictions from the theory of the asymmetric rotator.

The force constants are not unreasonable. The force between the base oxygens is about 5.5 times that between a base and the apical oxygen. The force constant between the base oxygens would predict a vibration frequency of these two atoms taken by themselves of about 2700 cm^{-1} whereas the vibration frequency of O_2 is 1580 cm^{-1}. It is well known that normal vibrations and interatomic distances follow the approximate law $r_e^n\omega_e$=constant where n lies between 2 and 3. In our case the figures lead to a value for n of 2.8. (The above argument must be regarded merely as an indication since the structures of O_2 and of O_3 may be quite dissimilar.)

The Raman spectrum of ozone is very weak and shows no lines which can be identified with certainty.[10,11] A molecule with an acute apical angle would not be expected to possess a strong Raman spectrum whereas one with an obtuse apical angle would.

There are only two experimental facts which do not appear to be in concordance with our interpretation of the spectrum. (*a*) The dipole moment of ozone is known to be small,[12] 0.49×10^{-18}. In general a molecule with an acute apical angle should exhibit marked polar qualities although in any particular case other circumstances might tend to reduce the dipole moment. (*b*) The electron diffraction measurements of Shand and Spurr indicate an apical angle of 127 degrees.

The experiment appears to have been carefully performed and we are unable to suggest any explanation for the discrepancy between the electron diffraction and the infra-red results. It is certainly true, however, that the infra-red spectrum of ozone cannot be identified as belonging to a molecule with an obtuse apical angle without the introduction of what seems to be an artificial series of assumptions and interpretations. It is believed that further precision measurements of the fine structure of the band at 14.2μ will definitely establish the moments of inertia of the molecule.

[10] G. B. B. M. Sutherland, Proc. Roy. Soc. **A141**, 515 (1933).
[11] G. B. B. M. Sutherland and S. L. Gerhard, Nature **130**, 241 (1932).
[12] G. L. Lewis and C. P. Smyth, J. Am. Chem. Soc. **61**, 3063 (1939).

Studies on Glass.

XVIII. The Heats of Solution of Crystalline and Glassy Glucose; the Heat of Mutarotation of α-Glucose

ROBERT D. ROWE AND GEORGE S. PARKS
Department of Chemistry, Stanford University, California

(Received March 12, 1946)

A calorimeter has been developed for the rapid solution of a powdered solid in a suitable solvent and the accurate determination of the heat of solution during the process. This calorimeter has now been used to determine the heats of solution of two preparations of crystalline α-*d*-glucose in water, both with and without mutarotation, and also the heats of solution of two preparations of glucose glass. Relatively accurate thermodynamic data for the crystal-to-glass transformation have been computed from these solution heats. Also small, but significant, differences per mole in enthalpy ($\Delta H_{298}=102\pm18$ cal.), in entropy ($\Delta S_{298}=0.24\pm0.06$ cal./deg.), and in free energy ($\Delta F_{298}^\circ=31\pm10$ cal.) have been found for these two glass preparations. A value of $\Delta H_{298}=-175$ (±5) calories has been obtained for the mutarotation of a mole of α-glucose, dissolved in water, to yield the equilibrium mixture of the alpha- and beta-forms.

INTRODUCTION

THE measurements here described were carried out during 1937–38 in order to provide as accurate data as possible concerning the relative heat contents of crystalline α-glucose and glassy glucose. The present results supersede the earlier, essentially preliminary, values of Parks, Snyder, and Cattoir.[1] Consequently, their thermodynamic calculations for the crystal-to-glass transformation are now revised in the light of these newer data.

When this investigation was started, it was also considered likely that the heat of solution of a sample of glucose glass would show variations with the history of its annealing, i.e., the time and temperature of storage, prior to the solution process itself, as previous measurements of the optical rotatory power[2] and the viscosity[3] of this material had disclosed rather appreciable changes with aging. No such effect was discernible, however, in the present study, probably because of the character of these solution experiments and the time requirements here involved.

Incidentally, the data for the heat of solution of the crystalline α-glucose in water, both with and without mutarotation, provide a new and relatively accurate value for the heat of mutarotation.

METHOD AND APPARATUS

After considerable preliminary experimentation, the "ordinary" method of calorimetry was adopted for measuring the heats of solution of the various glucose samples in water at approximately 25°C. With our final apparatus the actual solution process of the glucose, properly powdered, took place in about twenty seconds and complete thermal equilibrium was then attained two or three minutes later. The corrected temperature changes were readily computed by the Regnault-Pfaundler method from

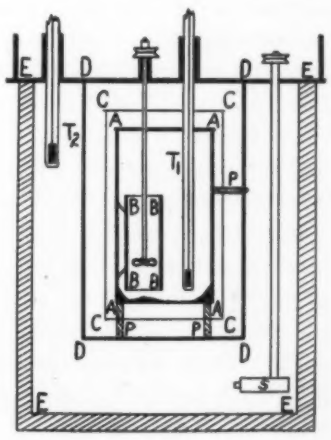

FIG. 1. A schematic diagram of the calorimetric assembly.

[1] G. S. Parks, L. J. Snyder, and F. R. Cattoir, J. Chem. Phys. **2**, 595 (1934).
[2] C. J. Jacobs and G. S. Parks, an unpublished study at Stanford University.
[3] G. S. Parks and J. D. Reagh, J. Chem. Phys. **5**, 364 (1937).

two series of temperature readings, taken for periods of twenty to thirty minutes prior to and immediately following each solution process.

Our calorimetric assembly, as finally developed, is represented schematically in Fig. 1. The calorimeter proper, designated by the lettering *AAAA*, was a cylindrical copper container of about 450-ml capacity, which had been given a number of coats of Bakelite varnish both inside and outside to protect the metal from alkaline reagents. It had a specially shaped, streamlined bottom and a tightly fitting lid. The stirrer was a four-bladed propeller of monel metal, operating in a small copper cylinder (*BBBB*) immersed in the solvent liquid and set off center in such a way as to circulate all of the liquid around the calorimeter thermometer (T_1) and the walls of the container. Evaporation was prevented by the tightly fitting lid, the special grease-filled seal on the stirrer shaft, and a rubber gasket about the thermometer. This container, the calorimeter, was surrounded by a silver shield (*CCCC*), in the form of a cylindrical can with a removable lid, to reduce radiation and convection effects and thus insure a small, uniform rate of heat transfer to or from the jacket, which in turn was a large copper can (*DDDD*) with a removable top. Six Bakelite pegs (only three are indicated in Fig. 1) supported both the convection shield and the calorimeter firmly, but in such a way that the latter could be easily removed. A special doorway, not shown in this figure, was provided through all three lids so that samples could be added with a minimum of heat transfer. These holes were closed by a removable, hollow outside door which supported covers for the convection shield and the inner calorimeter lid. A small spring on the support held the cover of this hole in the calorimeter lid tightly in place so as to prevent evaporation of the solvent.

The copper jacket, with the silver shield and calorimeter therein, was finally suspended within a fifteen-liter crock, which was filled with water at a temperature of about 24°C. A small rotary pump circulated the water in this crock, and both the jacket lid and hollow door were also filled with water. The entire apparatus was then placed in a thick-walled Celotex box with a removable Celotex cover. A 1/15 hp synchronous motor, connected by means of a system of belts and pulleys, drove the calorimeter stirrer and jacket circulating pump at constant speed, the former at 505 r.p.m. and the latter at 600 r.p.m.

The temperature changes within the calorimeter were measured to 0.0005° with a very fine Beckmann thermometer, manufactured specially for us by Max Tischer and Company (Ilmenau, Germany) and calibrated at 0.2° intervals by the Physikalisch-Technische Reichsanstalt. The jacket temperature was observed with an ordinary Beckmann thermometer (T_2). These thermometers were set at proper temperatures against a 0°–50° thermometer which had been calibrated to 0.01° by the National Bureau of Standards. This latter thermometer was also used to obtain the temperature of the samples and of the room during the experimental runs. Lens magnifiers were used in reading all thermometers.

The calibration of the calorimeter in the 22°–25° range was effectuated by a method of mixtures. In this calibration procedure a weighed sample of distilled water, initially at about 20°, was added to the calorimeter, which had been previously prepared by a partial filling with water and a temperature adjustment to 24° or 25°. By means of a copper-constantan thermocouple in conjunction with a White potentiometer, the temperature of this added water was measured to within 0.001° as it entered the calorimeter proper from a pipette. The final temperature of the calorimeter was then determined on its own Beckmann thermometer, against which the thermocouple had been standardized. Six such calibration experiments yielded a mean result of 62.0 calories per degree with a mean deviation of only ±0.3 calorie. This result checked roughly with a prior estimate of 59.2 calories per degree, exclusive of the heat capacity of the Beckmann thermometer, which had been made from the weights and known specific heats of the materials used in the construction of the calorimeter.

MATERIALS

Crystalline Glucose

Two preparations of crystalline α-*d*-glucose were employed in the present study.

The first material was a C. P. Pfanstiehl product, which was dried in a vacuum desiccator

over P_2O_5 for six weeks before use. It was then estimated to contain around 0.01 percent moisture in view of Jackson's observations.[4] An analysis by the polarimeter, based on the rotation data of Isbell and Pigman,[5] indicated that it was about 96 percent alpha- and 4 percent beta-glucose. This dried material was used in our initial measurements of the heat of solution of crystalline glucose and also in preparing the first sample of our glucose glass. Some of the undried crystals were likewise used in preparing the second sample of glass.

Our second crystalline material was some of Standard Sample No. 41, "Dextrose," as prepared by the National Bureau of Standards. It was a fine powder and was guaranteed to contain not over 0.01 percent moisture. Its initial rotation indicated that it was 100 percent α-glucose within the limits of error of our polarimetric measurements. This material was used in our final measurements of the heat of solution of crystalline α-*d*-glucose and its heat of mutarotation.

Glassy Glucose

As in other studies,[6] the preparations of glassy glucose were obtained by heating the crystalline Pfanstiehl glucose in a flask in a paraffin bath. The crystals melted at approximately 146°C and were then maintained under a vacuum at 155–160° for about five minutes, in order to eliminate bubbles of air or water vapor. When the liquid had become fairly clear, air was admitted and the material was allowed to cool to the glassy condition. To facilitate use in the solution experiments, the glass so prepared was next reduced to a powder by passing it through an old-fashioned, home meat grinder. This powder was then stored in vacuum desiccators over P_2O_5 until used.

Two batches of glassy glucose were prepared for the present measurements. Glass I was made from the remaining Pfanstiehl crystals which had been previously dried over P_2O_5 for six weeks. Glass II was made from similar undried material, which, however, should become completely freed of its water when heated above 150°C. Half of this latter glass preparation was kept at room temperature; the remainder was kept in the laboratory "cold room" at about 3°C.

THE HEATS OF SOLUTION

A uniform procedure was followed in measuring the heats of solution of these several glucose samples in water. Exactly 250 g of distilled water were first placed in the calorimeter and subsequently a portion of powdered glucose of 45.0 ($\pm$0.2) g mass was dissolved therein. Thus the resulting solution was always 1.00 molal.

The initial temperature of the calorimeter and solvent water in these experiments was about 24°C. The solution process for the crystals, being distinctly endothermic, resulted then in a temperature drop of 1.8 to 2.0°. On the other hand, the solution process of the glass was somewhat exothermic and yielded temperature rises of 0.8 to 1.0°. In the computations of the corresponding heat effects, the necessary values for the specific heat of water were taken from the International Critical Tables[7]; those for the glucose crystals and glass were derived from the preceding studies of Parks and co-workers.[8] In order to put all results on a truly comparable basis, the value for the changes in enthalpy (ΔH) in the solution process were finally adjusted to the standard temperature of 25° (i.e., 298°K) by taking $\Delta C_p = 0.20$ cal./g for the solution of the crystals and $\Delta C_p = 0$ for the solution of the glass. These ΔC_p values were based on the plausible assumption that the glucose in water constituted an almost ideal solution. The former value has also received excellent corroboration, subsequent to the completion of our work, from the measurements of Sturtevant,[9] who has shown that for the solution of alpha-crystals to a final concentration of approximately 0.2 molal $\Delta C_p = 0.200$ cal./g between 25° and 35°C. Our second value of $\Delta C_p = 0$ for the solution of the glass is of less importance, as the temperature adjustment to

[4] R. F. Jackson, Bureau of Standards Scientific Paper No. 293 (1916).
[5] H. S. Isbell and W. W. Pigman, J. Research Nat. Bur. Stand. **18**, 141 (1937).
[6] G. S. Parks and W. A. Gilkey, J. Phys. Chem. **33**, 1430 (1929); G. S. Parks, L. E. Barton, M. E. Spaght, and J. W. Richardson, Physics **5**, 193 (1934).
[7] *International Critical Tables* (McGraw-Hill Book Company, Inc., New York), Vol. VII, p. 232.
[8] G. S. Parks, H. M. Huffman, and F. R. Cattoir, J. Phys. Chem. **32**, 1366 (1928); G. S. Parks and S. B. Thomas, J. Am. Chem. Soc. **56**, 1423 (1934).
[9] J. M. Sturtevant, J. Phys. Chem. **45**, 127 (1941).

TABLE I. Heat of solution of Pfanstiehl *d*-glucose crystals at 25°C.

Experiment No.	Solvent	ΔH_{298} for solution (cal./g)
P-1	Pure water	14.63
P-2	Pure water	14.63
Mean without mutarotation	Pure water	14.63 (±0.02)
P-3	0.025*N* HCl	14.64
P-4	0.025*N* HCl	14.63
Mean	0.025*N* HCl	14.63 (±0.02)
P-5	0.0025*N* NH_4OH	13.99
P-6	0.0025*N* NH_4OH	13.97
P-7	0.0025*N* NH_4OH	13.96
P-8	0.0025*N* NH_4OH	13.91
Mean, incomplete mutarotation	0.0025*N* NH_4OH	13.96 (±0.03)
P-9	0.0050*N* NH_4OH	13.70
P-10	0.010*N* NH_4OH	13.74
P-11	0.020*N* NH_4OH	13.67
Mean with mutarotation		13.70 (±0.03)
Enthalpy change of mutarotation		$\Delta H_{298} = -0.93$ (±0.04)

25° in these cases involved an average interval of considerably less than one degree.

The solution experiments with the Pfanstiehl crystals were essentially preliminary and exploratory in character. These results are summarized in Table I. Experiments 1 and 2, carried out with pure water as solvent, yielded a value of $\Delta H_{298} = 14.63$ cal./g; and this result may be ascribed to the heat of solution of the material without mutarotation, as the crystals dissolved in less than twenty seconds and any subsequent, relatively slow mutarotation was automatically provided for in the derivation of the small, post-solution heating correction. The following pair of experiments with 0.025 normal HCl as solvent were expected to show at least some mutarotation effects, but apparently such a weak solution of hydrochloric acid is not an effective catalyst for the mutarotation process. Next, one to eight drops of concentrated ammonium hydroxide were added to the 250 g of solvent water to yield solutions ranging from 0.0025 up to 0.020 normal. The tabulated results show that in these cases the mutarotation process is apparently complete for our measurements with concentrations of, or above, 0.0050 normal.

Following these exploratory experiments, the heat of solution of the high grade *α-d*-glucose, prepared at the National Bureau of Standards, was measured in a first pair of determinations with pure water as solvent and in a second pair with 0.0125*N* NH_4OH as solvent. The results, representing the solution process both without and with mutarotation, are summarized in Table II.

A comparison of these values for the heat of solution of *α*-glucose with most of the earlier data in the literature is fraught with uncertainty, as several of these earlier investigators either overlooked the mutarotation problem or, at least, made inadequate allowance for its effect. Thus Barry's results,[10] adjusted by us to 25°C, are, respectively, $\Delta H_{298} = 15.04$ (±0.09) for solution of one gram of glucose in pure water to yield 0.2 molal concentration and $\Delta H_{298} = 14.90$ (±0.16) for corresponding solution in 1.64 normal hydrochloric acid, but he assumed that the heat of mutarotation was zero. Hendricks and co-workers[11] have also reported, without reference to possible mutarotation, 13.85 cal./g for the heat of solution of *α*-glucose in water at 21.6° to yield a 0.017 molal concentration; this result adjusts to $\Delta H_{298} = 14.53$ cal./g. The result of Parks, Snyder, and Cattoir,[1] which corresponds to $\Delta H_{298} = 14.72$ cal./g, probably involved very incomplete mutarotation, although these workers recognized the possible importance of this effect. The best published work to the present date appears to be that of Sturtevant[9] who has reported $\Delta H_{298} = 14.22$ (±0.02) cal./g for the solution of *α*-glucose, presumably without the mutarotation effect, in water to yield an approximately 0.2 molal concentration. His result is thus about 0.84 calorie below our present average for the non-mutarotated sugar. While his concentration differs considerably from ours, it is really hard to explain such a large difference in heat of solution.

Next, the heats of solution of preparations I and II of the glassy glucose were measured with 0.0125*N* NH_4OH as the solvent. This solvent was employed because the work of Jacobs and

TABLE II. Heat of solution of pure *α-d*-glucose crystals at 25°C.

Experiment No.	Solvent	ΔH_{298} for solution (cal./g)
BS-1	Pure water	15.090
BS-2	Pure water	15.041
Mean without mutarotation	Pure water	15.065 (±0.025)
BS-3	0.0125*N* NH_4OH	14.085
BS-4	0.0125*N* NH_4OH	14.116
Mean with mutarotation	0.0125*N* NH_4OH	14.100 (±0.015)
Enthalpy change of mutarotation		$\Delta H_{298} = -0.965$ (±0.030)

[10] F. Barry, J. Am. Chem. Soc. **42**, 1912 (1920).
[11] C. B. Hendricks, J. H. Dorsey, R. H. LeRoy, and A. G. Moseley, Jr., J. Phys. Chem. **34**, 418 (1930).

Parks[2] had indicated that such glucose glass preparations represent a mixture of the alpha- and beta-forms, and hence it seemed desirable to ensure here a final solution of mutarotated product comparable to that obtained when the crystals of α-glucose were previously dissolved in a mutarotating solvent. Our various results with the two glasses, as these were subjected to an aging treatment of from one to sixteen days, have been summarized in Table III. From these data it is noticeable that the heats of solution of Glass I averaged about 10 percent greater (numerically) than those of Glass II.

However, the aging process at 24°C had no appreciable effect on the character of our results, nor did the storage of samples of Glass II for thirteen days at 3° produce any significant change in its heat content as we measured this quantity. Previously, Parks and Reagh[3] had observed very appreciable changes in the viscosity of glucose threads when these were aged in the neighborhood of 20° to 30°; and more recently Nelson and Newton[12] have found that the average specific heat between 25° and 30° for a sample of glucose glass increased about 15 percent when stored at 25° for seven days. In view of our present results, it would seem that any appreciable changes in the enthalpy of these glasses with aging must have developed largely within the first twenty-four hours. Moreover, our experimental method, which involved maintaining the glucose glass samples for one or two hours around 24° prior to a solution determination but following the storage for thirteen days at 3°, apparently precluded the observation of such a change of heat content as was noted by Nelson and Newton in their specific heat study.

TABLE III. Heat of solution of glassy glucose samples in 0.0125N NH_4OH at 25°C.

Experiment No.	Age of sample in days*	ΔH_{298} for solution (cal./g) Glass I	Glass II
GG-1	1	−6.15	—
GG-2	1	−6.22	—
GG-3 and 6	2	−6.07	−5.62
GG-7	2	—	−5.62
GG-8	2	—	−5.58
GG-4	3	−6.27	—
GG-5	3	−6.21	—
GG-9	11	−6.25	—
GG-10	11	−5.98	—
GG-11 and 13	15	−6.00	−5.56*
GG-12 and 14	15	−6.08	−5.62*
GG-15	16	—	−5.61
GG-16	16	—	−5.51
Mean result		−6.14 (±0.09)	−5.57 (±0.05)

* The aging of samples was carried out at a temperature of 24°C except in Experiments *GG*-13 and 14. These two samples of Glass II were aged for 13 days at 3° prior to the solution experiments.

THERMODYNAMIC CALCULATIONS FOR THE CRYSTAL-TO-GLASS TRANSFORMATION

The thermodynamics of the crystal-to-glass transformation have been previously considered by Parks, Snyder, and Cattoir,[1] but our new data now provide a more accurate basis for such a study with two somewhat different glass preparations.

From the mean results for Glass I in Table III and for the crystals with mutarotation in Table II the enthalpy difference is 20.24 (±0.10) cal./g at 25°C. This yields for the molal process

$$C_6H_{12}O_6\ (\alpha\text{-crystals}) \rightarrow C_6H_{12}O_6\ (\text{glass});$$
$$\Delta H_{298} = 3646\ (\pm 18)\ \text{cal.} \quad (1)$$

Above 25°C the glass softens and in the neighborhood of 40° the product in this process becomes obviously a very viscous liquid. An examination of the available specific heat data[8,12] for crystalline and undercooled liquid glucose indicates that the difference between the heat capacity of the undercooled liquid and the crystalline form is almost independent of the temperature; and accordingly we shall now take the value $\Delta C_p = 35$ cal. per mole between 25° and 146° (the melting point of pure α-glucose crystals). Hence, by Kirchhoff's law, we can calculate for the conversion of a mole of α-crystals into liquid glucose at 146°C

$$\Delta H_{419} = 3646 + 35\ (146-25)$$
$$= 7881\ (\pm 100)\ \text{cal.} \quad (2)$$

This result for the heat of fusion of α-glucose crystals is in fairly good agreement with the experimental one obtained by Thomas and Parks[8] with their radiation calorimeter. Their value for a glucose sample, somewhat contaminated with decomposition products, was 41.7 cal. per gram at 141°, which corresponds to about 7685 cal. per mole at 146°C.

The entropy increase on fusion of the α-crystals

[12] E. W. Nelson and R. F. Newton, J. Am. Chem. Soc. 63, 2178 (1941).

TABLE IV. Thermodynamic data for the transformation α-glucose crystals→glassy glucose, per mole.

	Glass I	Glass II	Glass P-S-C
ΔH_{298} in calories	3646	3544	3893
ΔS_{298} in cal./°K	6.87	6.63	7.46
$\Delta F_{298}°$ in calories	1598 (±15)	1567 (±15)	1669 (±50)
ΔH_{419} in calories	7881	7779	8128
ΔS_{419} in cal./°K	18.80	18.56	19.39
$\Delta F_{419}°$ in calories	0	0	0

at 146° follows directly from the data of Eq. (2):

$$\Delta S_{419} = 7881/419 = 18.80 \text{ e.u.} \quad (3)$$

The entropy change for the hypothetical conversion of a mole of the crystals into glucose glass at 25°C can be evaluated next with the aid of the ΔC_p value used previously:

$$\Delta S_{298} = 18.80 - 35 \ln (419/298) = 6.87\ (\pm 0.07) \text{ e.u.} \quad (4)$$

By means of the fundamental thermodynamic equation $\Delta F = \Delta H - T\Delta S$, and the data of Eqs. (1) and (4), we can then obtain the molal free energy change for the crystal-to-glass transformation at 25°C:

$$\Delta F_{298}° = 1598\ (\pm 15) \text{ cal.} \quad (5)$$

It may be noted that the relatively small uncertainty in this final free energy value is a consequence of a compensative effect in the corresponding uncertainties for the ΔH_{298} and ΔS_{298} values.

Similar data have also been worked out for the case of Glass II, and the preliminary results of Parks, Snyder, and Cattoir have now been revised with 35 for ΔC_p instead of the value of 33 calories per degree, which was originally used. The thermodynamic values for the three glasses are here summarized in Table IV to facilitate comparisons.

From these tabulated data we obtain for the hypothetical transformation, per mole,

Glass I→Glass II,

$\Delta H_{298} = -102\ (\pm 18)$ cal.;

$\Delta S_{298} = -0.24\ (\pm 0.06)$ e.u;

and

$$\Delta F_{298}° = -31\ (\pm 10) \text{ cal.}$$

Here the uncertainties are those which exist after the elimination of possible systematic errors, common to the data for both glasses and canceling in a transformation of this type.

Such results strongly support the concept of *a series of glassy states* for a substance, with appreciably different enthalpy and free energy contents, as previously suggested by Parks and Reagh.[3]

THE HEAT OF MUTAROTATION OF ALPHA-GLUCOSE

Our data in Tables I and II provide new values for the enthalpy change when a mole of α-*d*-glucose, dissolved in water, is transformed into an equilibrium mixture of the alpha- and beta-forms. By use of the optical rotation values of Isbell and Pigman[5] we estimate that such an equilibrium solution contains 63.6 percent beta- and 36.4 percent alpha-glucose at 25°C. As our Pfanstiehl crystals initially appeared to be only about 96.0 (±1.0) percent α-glucose, we now calculate from Table I, for the mutarotation effect starting with a mole of pure α-glucose,

$$\Delta H_{298} = -(0.93)(180.156)(63.6/59.6) = -178\ (\pm 8) \text{ cal.}$$

Likewise, from the solution data for the pure alpha-crystals of Table II we obtain a somewhat more reliable value of

$$\Delta H_{298} = -(0.965)(180.156) = -174\ (\pm 5) \text{ cal.}$$

Accordingly, as a final, weighted mean we shall take $\Delta H_{298} = -175\ (\pm 5)$ calories per mole.

As noted in the previous discussion of the heats of solution of glucose crystals, several of the earlier investigators either overlooked this heat effect in mutarotation or assumed that it was zero. Brown and Pickering,[13] however, obtained a value of 106 cal. per mole in 1897 and Sturtevant[14] reported 162 (±4) cal. in 1937. More recently, in a second paper[9] dealing with precise calorimetry, he has found a result of 174.2 (±0.9) cal., which agrees excellently with our final value of 175 (±5) calories for this mutarotation process.

[13] H. T. Brown and S. Pickering, J. Chem. Soc. **71**, 756 (1897).

[14] J. M. Sturtevant, J. Am. Chem. Soc. **59**, 1528 (1937).

A Relation between Internuclear Distances and Potential Barriers of Methyl Groups

F. A. FRENCH* AND R. S. RASMUSSEN
Shell Development Company, San Francisco and Emeryville, California

(Received March 18, 1946)

An empirical relation is shown between contributions of various groups to the potential barriers of methyl groups and the minimum distance of approach of atoms of these groups to the methyl group. The use of this relation to derive barrier values for other molecules is demonstrated.

I. INTRODUCTION

THE existence of barriers hindering the rotation of groups about bonds has been known for some time. Methods have been described for the calculation of these potential barriers by the comparison of the results of thermodynamic measurements with the results of statistical mechanical calculations.[1]

A method of estimating potential barriers where no thermodynamic data exist is highly desirable for the calculation of thermodynamic functions. The available evidence indicates that the equilibrium configuration of groups on opposite ends of a CC axis is staggered rather than opposed.[2] A plausible explanation of the origin of these barriers is that they arise from repulsive forces between the atoms of the groups in relative rotation. In the barriers considered here (methyl groups rotating on various molecular frames) these forces are presumably of the Van der Waals type, operating between the CH bonding electrons of the methyl group and the other atoms of the molecule.[3]

It may be possible that energy *vs.* distance relationships, similar to the usual type of interatomic energy curves, exist for pairs of atoms on opposite ends of a bond about which rotation is occurring. From such curves it would then be possible to calculate the energy changes which occur when groups rotate relative to one another. This approach was used in a recent paper by Aston, Isserow, Szasz, and Kennedy.[4] An interatomic potential of the form $V=k/r_{ij}^n$ was assumed between pairs of atoms ij. The constants were evaluated from known barriers in ethane and neopentane and other barriers were calculated with fair success. A simpler and more empirical approach has been adopted by the present authors. This method reproduces the barriers of methyl groups in a certain class of molecules with somewhat greater accuracy and is easier to apply.

As is the common practice, the assumption of independence of torsional coordinates is made, i.e., the absence in the potential energy function of cross terms involving products of torsional coordinates of different groups. Although such cross terms, particularly between adjacent torsional rotators, certainly do exist and have been evaluated for one simple case (see Pitzer, reference 6), the difficulty of their evaluation and the fact that they would seem to be small compared to the "pure" potential terms have led to the use of effective barriers obtained by ignoring them.

II. DEPENDENCE OF BARRIERS ON MINIMUM INTERNUCLEAR DISTANCES

The barrier on a single methyl group is regarded as being due to a summation of contributions from interactions with groups on the other end of the rotational axis. For example, the

* Present address: Harold Brunn Research Institute, Mt. Zion Hospital, San Francisco, California.

[1] K. S. Pitzer and W. D. Gwinn, J. Chem. Phys. **10**, 428 (1942). This is the most recent paper on the theory and gives references to earlier work.

[2] V. Schomaker and D. P. Stevenson, J. Chem. Phys. **8**, 637 (1940); K. W. F. Kohlrausch and H. Wittek, Zeits. f. physik. Chemie **B48**, 177 (1941).

[3] Effects due to unshared electron pairs have been ignored. The ultimate justification for this lies in the success achieved when only hydrogen-hydrogen interactions are considered. In other cases than those considered here it may be necessary to take into account the additional effect of dipole-dipole interactions: J. Y. Beach and D. P. Stevenson, J. Chem. Phys. **6**, 635 (1938); J. Y. Beach and K. L. Palmer, J. Chem. Phys. **6**, 639 (1938).

[4] J. G. Aston, S. Isserow, G. J. Szasz, and R. M. Kennedy, J. Chem. Phys. **12**, 336 (1944).

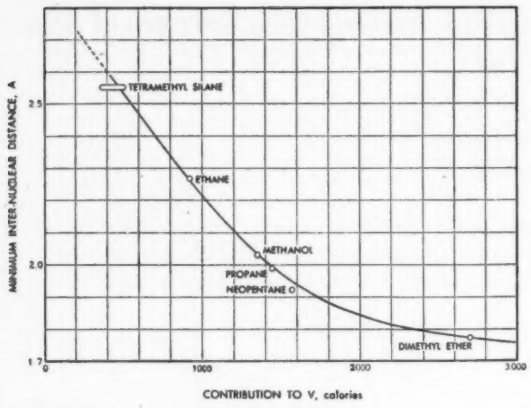

FIG. 1. Relation of barrier contributions to minimum internuclear distance.

barrier of 2750 calories found for ethane[5] may be looked upon as three times the barrier offered to a methyl group by a single CH bond at the other end of the CC rotation axis. Hence, this barrier contribution may be taken as 920 cal. The observed barrier of 3300 cal. restricting the rotation of a methyl group in propane[6] may be regarded, similarly, as being a summation of two 920-cal. contributions from the hydrogen atoms on the central carbon atom and a contribution due to the other methyl group. Thus this contribution has a value of $3300-2\times920=1460$ cal. The observed barriers to the methyl group rotations in methanol and dimethyl ether may be regarded as being entirely due to the hydrogen atom and the methyl group, respectively, while those in neopentane and tetramethylsilane are three times the individual contribution from a methyl group on the other end of the rotation axis.

The minimum distance of approach of a hydrogen nucleus of the methyl group to any hydrogen nucleus on the opposing group has been chosen as a convenient measure of the amount of interaction giving rise to a barrier contribution. This minimum distance of approach is taken with respect to the rotation of the groups with all parameters other than rotational orientation held constant. Thus for ethane the minimum distance is that from a hydrogen nucleus on one end to the corresponding hydrogen nucleus on the other end of the CC axis when the groups are in the opposed (D_{3h}) configuration. For propane the minimum distance between methyl groups is calculated with both methyl groups in the "opposed" configuration with respect to the CH_2 group. Other molecules are treated in a similar fashion. When these minimum distances are plotted against the barrier contributions from the respective groups, the points may be fitted remarkably well by a single smooth curve (Fig. 1). It is an oversimplification to assert that all the forces giving rise to the barrier are functions of this single parameter; nevertheless the excellence of the fit and the adequacy of the predictions made from the curve indicate that this parameter (minimum distance of approach) is a useful measure of the magnitude of the interactions of the groups involved.

The barriers used in obtaining data for the construction of Fig. 1 are listed in Table I. All values given are taken directly from the indicated literature references with the exception of the one for dimethyl ether, which together with methanol requires special discussion.

For methanol an analysis of the fine structure of the infra-red absorption spectrum by Koehler and Dennison[7] led to an estimate of 1340 calories for the barrier. Crawford[8] calculated a barrier of 3400 calories using the third law entropy obtained for liquid methanol by Kelley[9] and the

TABLE I. Barrier contributions used in construction of Fig. 1.

Compound	Measured barrier, cal.	Distances, A	Barrier contributions, cal.	References
Ethane	2750	2.270	920	5
Propane	3300	2.261, 1.991	930, 1440	6, *a*
Neopentane	4800	1.923	1570	*b*
Methanol	1350	2.030	1350	7
Tetramethylsilane	1100–1500	2.556	370–500	*c*
Dimethyl ether	2700	1.774	2700	see text

[a] The values shown here for barrier contributions differ very slightly from those used in the text. This is due to a slight adjustment made in the methyl-to-methylene closest hydrogen distance, resulting from the non-tetrahedral angles about the central carbon, and making this distance somewhat shorter than the analogous ethane distance.
[b] J. G. Aston and G. H. Messerly, J. Am. Chem. Soc. **58**, 2354 (1936); K. S. Pitzer, J. Chem. Phys. **5**, 473 (1937); K. S. Pitzer, Chem. Rev. **27**, 39 (1940).
[c] J. G. Aston, R. M. Kennedy, and G. H. Messerly, J. Am. Chem. Soc. **63**, 2343 (1941).

[5] G. B. Kistiakowsky, J. R. Lacher, and F. Stitt, J. Chem. Phys. **7**, 289 (1939).
[6] G. B. Kistiakowsky and W. W. Rice, J. Chem. Phys. **8**, 610 (1940). A value of 3400 cal. was recently derived by K. S. Pitzer, J. Chem. Phys. **12**, 310 (1944).
[7] J. S. Koehler and D. M. Dennison, Phys. Rev. **57**, 1006 (1940).
[8] B. L. Crawford, Jr., J. Chem. Phys. **8**, 744 (1940).
[9] K. K. Kelley, J. Am. Chem. Soc. **51**, 181 (1929).

latent heat of vaporization measurements of Fiock, Ginnings, and Holton.[10] However, since methanol has only a single hydrogen-methyl interaction at each maximum, it would be expected to have a barrier much smaller than that of ethane where three interactions contribute to each maximum. Much higher latent heats than those of Fiock, Ginnings, and Holton, which are *a priori* as acceptable, have been reported in the literature.[11] Third law entropies calculated using these data give a barrier in close agreement with the spectroscopic value of 1340 calories. For these calculations the frequency assignment of Noether[12] and the moments of inertia shown in Table II were used. Consequently, the spectroscopic value was adopted. Since there has been considerable lack of agreement on the barrier for this molecule, the data referred to above are discussed in detail in an appendix to this paper.

For dimethyl ether an accurate third law entropy has been determined by Kennedy, Sagenkahn, and Aston.[13] Using the frequency assignment of Crawford and Joyce[14] they obtained a barrier of 3100 cal. Unpublished infra-red data from these laboratories led to a frequency assignment sufficiently different from that of Crawford and Joyce to warrant recalculation of the barrier, leading to a value of 2700 cal. This frequency assignment together with the moments of inertia used is shown in Table II. The heat capacity data of Kistiakowsky and Rice[15] on dimethyl ether vapor unfortunately cannot be used to determine the barrier, since contributions from the internal rotations in the temperature range of the measurements are nearly constant over a fairly broad range of barrier values. Small errors in either the frequency assignment or the heat capacity measurements would lead to large errors in the barrier. However, the calculated and observed heat capacities are in substantial agreement. Consequently the value of 2700 calories was accepted.

TABLE II. Moments of inertia and vibrational frequencies used in statistical calculations.

Compound	Product of moments of inertia, g^3 cm^6	Reduced moment for internal rotation, g cm^2	Vibrational frequencies, cm^{-1}
Dimethyl ether	$1.708 \cdot 10^{-115}$	$4.33 \cdot 10^{-40}$	412, 920, 1102, 1180(2), 1260(2), 1425(2), 1450(2), 1462(2), 2930(6)
Methanol	$7.748 \cdot 10^{-117}$	$1.08 \cdot 10^{-40}$	1034, 1209, 1260, 1340, 1430, 1455, 1477, 2845, 2978(2), 3683
Methylamine	$1.101 \cdot 10^{-116}$	$1.82 \cdot 10^{-40}$	620, 783, 1064, 1120, 1174, 1426, 1460(2), 1625, 2930(3), 3350(2)
Acetone	$1.398 \cdot 10^{-111}$	$4.99 \cdot 10^{-40}$	391, 488, 531, 787, 900(2), 1066, 1070, 1220, 1350, 1353, 1420, 1423, 1430 1438, 1710, 2930(6)
Dimethyl sulfide	$7.867 \cdot 10^{-115}$	$4.90 \cdot 10^{-40}$	Same as those of Osborne, Doescher, and Yost.[a]

All physical constants used were taken from R. T. Birge, Rev. Mod. Phys. **13**, 233 (1941). Thermodynamic contributions for restricted rotators were from the tables of Pitzer and Gwinn, reference 1.
[a] Osborne, Doescher, and Yost, J. Am. Chem. Soc. **64**, 169 (1942).

The molecular constants used in calculating the minimum internuclear distances used in Fig. 1 are given in Table III. The CH bond length of 1.093A from spectroscopic work on methane[16] and the CC bond distance of 1.542A from x-ray diffraction work on diamond[17] were used throughout. The bond angles in methyl groups were assumed to be tetrahedral. All other values used and their sources are indicated in Table III. Interatomic distances were carried to 0.001A in all cases. This is well beyond the accuracy with which these parameters are known for most molecules. However, since small changes in these distances were significant, this procedure gave a greater degree of internal consistency than would have been obtained with values rounded off to the experimentally significant limit of 0.01A.

III. TESTS OF THE METHOD

A number of calculations have been made to illustrate the use of the curve of Fig. 1 in esti-

[10] E. F. Fiock, D. C. Ginnings, and W. B. Holton, Bur. Stand. J. Research **6**, 881 (1931).
[11] E. Bartoszewicz, Rocznicki Chem. **11**, 90 (1931); Chem. Abs. **25**, 5343 (1931); S. Young, Proc. Roy. Dublin Soc. **12**, 374 (1911).
[12] H. D. Noether, J. Chem. Phys. **10**, 693 (1942).
[13] R. M. Kennedy, M. Sagenkahn, and J. G. Aston, J. Am. Chem. Soc. **63**, 2267 (1941).
[14] B. L. Crawford, Jr. and L. Joyce, J. Chem. Phys. **7**, 307 (1939).
[15] G. B. Kistiakowsky and W. W. Rice, J. Chem. Phys. **8**, 618 (1940).
[16] D. M. Dennison, Rev. Mod. Phys. **12**, 210 (1940).
[17] Value given by L. Pauling, *Nature of the Chemical Bond* (Cornell University Press, Ithaca, 1939), first edition, p. 150.

TABLE III. Molecular structural parameters used in calculating minimum distances of approach of rotating groups.

Molecule	Parameters (lengths in A)
Ethane	standard values (see text)
Propane	<CCC, 111° 30′
Neopentane	standard values; <CCC tetrahedral
Methanol	CO, 1.420; OH, 0.959; <COH, 104° 40′
Tetramethylsilane	CSi, 1.93; <CSiC tetrahedral
Dimethyl ether	CO, 1.420; <COC, 111°
Methylamine	CN, 1.470; NH, 1.016; <CNH, 108°; <HNH, 108°
Dimethylamine	CN, 1.470; NH, 1.016; <CNH, 108°; <CNC, 110°
Trimethylamine	CN, 1.470; <CNC, 110°
Methyl mercaptan	CS, 1.82; SH, 1.35; <CSH, see text, Section III
Dimethyl sulfide	CS, 1.82; <CSC, 96°
Acetone	CO, 1.21; CC, 1.52; <CCC, 120°
Isobutane	<CCC, 111° 30′
Trimethylborane	BC, 1.56; <CBC, 120°
Trimethylphosphine	PC, 1.87; <CPC, 100°
Methyl hydroselenide	CSe, 1.93; SeH, 1.49; <CSeH, 90°
Methyl hydrotelluride	CTe, 2.10; TeH, 1.68; <CTeH, 90°
Tetramethylgermane	CGe, 1.98; <CGeC tetrahedral
Tetramethyltin	CSn, 2.18; <CSnC tetrahedral
Tetramethyllead	CPb, 2.23; <CPbC tetrahedral

These parameters were taken from the electron diffraction results summarized by: L. Pauling, *Nature of the Chemical Bond* (Cornell University Press, Ithaca, 1939), first edition, Chaps. III and V. V. Schomaker and D. P. Stevenson, J. Am. Chem. Soc. **63**, 37 (1941).

In addition, spectroscopic results were utilized for certain of the parameters of methanol (OH distance; see A. Borden and E. F. Barker, J. Chem. Phys. **6**, 553 (1939)), the amines (NH distance and HNH angle taken from NH_3), and methyl mercaptan (SH distance taken from H_2S).

mating barriers and to demonstrate the accuracy and practicality of this method. The comparisons of estimated barriers and those reported in the literature, for molecules other than those used in constructing the curve, are given in Table IV. In addition the potential barriers have been estimated for a number of molecules that are amenable to statistical treatment and for which no calorimetric measurements have been published. Molecular constants used in calculating minimum internuclear distances for these molecules are given in Table III.

The following discussion of the check calculations will illustrate the method as applied to the methylamines, methyl mercaptan, dimethyl sulfide, acetone, and isobutane.

The closest distance of approach of a methyl-group hydrogen to the hydrogen of an NH group linked to the methyl is 2.151A, using the molecular dimensions in Table III for methylamine. Therefore, from Fig. 1, the barrier contribution of the NH bond is 1110 cal. The closest distance between a methyl-group hydrogen and a hydrogen of another methyl-group bonded to the same nitrogen atom is 1.823A, leading to a contribution of 2130 cal. offered by the $-NCH_3$ group to a methyl group in di- and trimethylamine. A small expansion of the CNC angle over the HNH angle was assumed for di- and trimethylamine analogous to the known increase in the CCC angle of hydrocarbons over the tetrahedral value. Summing the contributions from the proper groups, the following barriers are obtained for methyl groups in the methylamines:

$$\text{monomethylamine} = 2\times 1110 = 2220 \text{ calories},$$
$$\text{dimethylamine} = 1130 + 2130, = 3260 \text{ calories},$$
$$\text{trimethylamine} = 2\times 2130 = 4260 \text{ calories}.$$

These values are in close agreement with experimentally determined values, as shown in Table IV.[18]

The third law entropy of methyl mercaptan leads to a barrier of 1460 calories. The value from Fig. 1 is 930–1010 depending on the CSH angle assumed. In the case of dimethyl sulfide, while an accurate third law entropy has been determined, the uncertainty in the CSC angle makes an accurate determination of the barrier impossible. Using an angle of 96° for calculation of the moments of inertia leads to a barrier of 1990 calories for each methyl group. This same angle gives a minimum hydrogen-hydrogen distance between methyl groups of 1.867A and a barrier of 1870 calories from Fig. 1, in satisfactory agreement.

In the case of acetone, the third law entropy of the liquid,[19] various reported heats of vaporization, the heat capacity of the gas,[20] and the frequency assignment shown in Table II gave barriers ranging from 560 to 1240 calories compared to 970 calories from Fig. 1.

For isobutane the third law entropy led to a barrier of 3870 calories.[21] Using a CCC angle of 111°30′ a barrier of 3850 calories was obtained from Fig. 1.

[18] Using the gaseous heat capacity data of Felsing and Jesson, J. Am. Chem. Soc. **55**, 4418 (1933), and the frequency assignment for methylamine given in Table II, values of C_p(calc.)$-C_p$(obs.) of +.59 at 0°C, −.05 at 25°C, and −.52 at 50°C were obtained. A similar trend was noticed by Aston, Eidinoff, and Forster, J. Am. Chem. Soc. **61**, 1539 (1939), in comparing calculated and observed C_p's of Felsing and Jesson for dimethylamine. These trends cannot be accounted for by any reasonable modifications of barrier or frequency assignments.

[19] K. K. Kelley, J. Am. Chem. Soc. **51**, 1145 (1929).

[20] K. Bennewitz and W. Rossner, Zeits. f. physik. Chemie **B39**, 126 (1938).

[21] J. G. Aston, R. M. Kennedy, and S. C. Schumann, J. Am. Chem. Soc. **62**, 2059 (1940).

IV. APPLICATION TO OTHER CLASSES OF MOLECULES

This method for estimating barriers is, as emphasized above, applicable only to methyl groups, since it is only by virtue of the threefold symmetry that it becomes legitimate to split the barrier up into independent contributions from the groups giving rise to the barrier. However, some fairly successful attempts have been made to estimate barriers for other simple groups bearing hydrogens.

Thus in ethanol the methyl-group barrier was calculated from the interactions with two methylene-group hydrogens at 2.270A and one-third of the contribution from the hydroxyl hydrogen, whose closest approach is at 1.798A. Similarly, the barrier for the OH group was calculated from Fig. 1, using an average of values obtained from the minimum distances of approach of the OH hydrogen to the methylene-group hydrogens and to the nearest methyl-group hydrogen:

$$V_{OH}=\frac{2400+2\times1340}{3}=1690 \text{ cal.}$$

$$V_{Me}=2\times916+\frac{2400}{3}=2630 \text{ cal.}$$

In isopropyl alcohol the analogous values are $V_{OH}=2070$, $V_{Me}=3240$, and in tertiary butyl alcohol $V_{OH}=3400$ and $V_{Me}=4010$. These values for the OH group barriers are believed to be reliable. If, however, the oxygen atom has any large effect the methyl barrier estimates may be low. Preliminary comparisons of statistical calculations for these alcohols with the results of all known measurements are satisfactory. The data on these alcohols are from various sources, which are often in serious disagreement. Hence, a complete treatment of the data, which will be presented in a later paper, is required to clarify the picture.

In molecules such as butane where the rotating groups are highly unsymmetrical the present method does not seem to be applicable, and in such cases it will probably be necessary to use a more difficult but more fundamental treatment such as that of Aston.

A consideration of the barriers hindering the rotation of methyl groups attached to ethylenic frames has been omitted from this correlation for several reasons. In the rotation of these groups there may be six maxima per rotation and the barrier contributions might be expected to be different from those predicted from Fig. 1, which was constructed from data on molecules having three maxima per rotation.

TABLE IV. Barriers derived from Fig. 1, and comparison with experimental values.

Compound	Distances, A	Contributions from Fig. 1, cal.	Total barrier from contributions, cal.	Measured barrier, cal.	References
Methylamine	2.151	1110	2220	1520 or more	*a*
Dimethylamine	2.140, 1.823	1130, 2130	3260	3460	*b*
Trimethylamine	1.823	2130	4260	4270	*c*
Methyl mercaptan	2.208–2.262*	1010–930	1010–930	1460	*d*
Dimethyl sulfide	1.867**	1870	1870	2000	*e*
Acetone	2.271	920	920***	560–1240	see text, Section III
Isobutane	2.232, 1.991	970, 1440	3850	3870	*f*
Trimethylborane	2.302	860	1720		
Trimethylphosphine	2.098	1210	2420		
Methyl hydroselenide	2.340	800	800		
Methyl hydrotelluride	2.548	470	470		
Tetramethylgermane	2.638	~400	~1200		
Tetramethyltin	2.965	~0	~0		
Tetramethyllead	3.046	~0	~0		

* Assuming a CSH angle of 90° and 92° 20′, respectively.
** Assuming a CSC angle of 96°.
*** Assuming the whole barrier to be due to the other methyl group. The barrier derived on this assumption fits the available experimental data within their probable errors.
a J. G. Aston, C. W. Siller, and G. H. Messerly, J. Am. Chem. Soc. **59**, 1743 (1937); J. G. Aston and P. M. Doty, J. Chem. Phys. **8**, 743 (1940).
b J. G. Aston, M. L. Eidinoff, and W. S. Forster, J. Am. Chem. Soc. **61**, 1539 (1939).
c J. G. Aston, M. L. Sagenkahn, G. J. Szasz, G. W. Moessen, and H. F. Zuhr, J. Am. Chem. Soc. **66**, 1171 (1944).
d H. Russell, Jr., D. W. Osborne, and D. M. Yost, J. Am. Chem. Soc. **64**, 165 (1942).
e D. W. Osborne, R. N. Doescher, and D. M. Yost, J. Am. Chem. Soc. **64**, 169 (1942).
f J. G. Aston, R. M. Kennedy, and S. C. Schumann, J. Am. Chem. Soc. **62**, 2059 (1940).

V. CONCLUDING REMARKS

This method, like any other method of estimating barriers based on an exact knowledge of interatomic distances, is very sensitive to changes in these parameters, particularly in the region of short internuclear distances. For this reason an effort has been made to use a consistent set of molecular constants. Values consistent with those which entered into the construction of Fig. 1 must be used in making barrier estimates from this curve. The arbitrariness in the choice of molecular constants is particularly evident in the choice of hydrogen angles. It is impossible, at present, to state the precise values for these angles in complex molecules because they cannot be obtained by current spectroscopic and electron diffraction methods. It has been assumed, for example, that the COH angle is the same as the water angle and that HCC and HCH angles are tetrahedral, except in cases where this is obviously untrue (such as the HCC angle of the tertiary hydrogen in isobutane).

An additional point of question lies in the uncertainties of the values of the barriers used in constructing Fig. 1. These uncertainties may, in some cases, be as high as ±500 calories. However, the excellence of fit of the barrier contributions to a smooth curve, and the relatively small deviations between the barriers estimated from the curve and those estimated by the usual methods from calorimetric data indicate that this method will yield values which are entirely adequate for practical thermodynamic calculations.

The concept that repulsive forces give rise to potential barriers in the types of molecules considered is supported further by the electron diffraction evidence that CCC angles are greater than tetrahedral in propane, isobutane, and tertiary butyl chloride.[22] In addition the change in some methyl rocking frequencies from approximately 1160 wave numbers in methyl groups attached to secondary and tertiary C atoms to approximately 1250 in methyl groups attached to quaternary C atoms is readily interpreted as being due to the increased repulsion from adjacent groups.

[22] L. Pauling and L. O. Brockway, J. Am. Chem. Soc. **59**, 1223 (1937); J. Y. Beach and D. P. Stevenson, J. Am. Chem. Soc. **60**, 475 (1938); J. Y. Beach and J. Walter, J. Chem. Phys. **8**, 303 (1940).

APPENDIX: THE BARRIER IN METHANOL

The entropy of methanol vapor at 298.16°K and one atmosphere can be derived from available data as follows:

Entropy of liquid, 298.16°K (Kelley[9])	30.26 e.u.
Entropy of vaporization[10,11]	30.015, 30.447, 30.688
Gas imperfection correction (Berthelot Eq.)	0.02
Entropy change, vapor pressure to one atmos.	−3.586
Entropy of vapor at 298.16°K and one atmos.	56.71, 57.14, 57.38 e.u.

The three values given for entropy of vaporization are those derived from the latent heat values of Fiock, Ginnings, and Holton,[10] Young,[11] and Bartoszewicz,[11] respectively. These values are 8949.4 cal., 9078 cal., and 9150 cal.

The statistically calculated entropy, except for the internal rotational contribution, is (using constants and frequencies shown in Table II):

Vibrational	0.220 e.u.
Translational-rotational	55.291
	55.511 e.u.

Thus the contribution from internal rotation is 1.20, 1.63, or 1.87 e.u., respectively, obtained from the three latent heat values. The first value, 1.20 e.u., derived from the Fiock, Ginnings, and Holton datum, leads to a barrier of 2360 cal. The spectroscopic value for the barrier (1340 cal.) gives an internal rotational contribution of 1.65 e.u., in essential agreement with the latter two values. The discrepancy between the barrier (2360 cal.) derived here using the Fiock, Ginnings, and Holton latent heat and that given by Crawford[8] (3400 cal.) derived from the same latent heat and liquid entropy is due mainly to the more recent physical constants and frequency values used here.

Force Constant of the Association Bond in the Formic and Acetic Acid Dimers

J. O. HALFORD
Department of Chemistry, University of Michigan, Ann Arbor, Michigan

(Received April 4, 1946)

The entropies of the formic and acetic acid dimers are used to find a minimum value for the force constant of the association bond. With the aid of a normal coordinate treatment the probable value is found to be 4×10^4 dynes/cm. This agrees with a rough estimate from the heat of dimerization. A Raman band in the formic acid spectrum at 200 cm^{-1} may be due to the association vibrations.

IN earlier papers,[1] the calculation of reasonably accurate entropies from vapor densities, vapor pressures, and thermal data has been described for the momomers and dimers of formic acid and acetic acid. The dimer entropies, for the hypothetical perfect gases at 25°C and atmospheric pressure, were found to be 83.1 ± 0.1 and 101.0 ± 0.3 e.u., respectively, for the two acids.

These entropies may be used to estimate the stretching force constant of the hydrogen bonds by which the two monomer units are thought to be held together in the dimer. The procedure is to find the entropy and frequency of the symmetrical vibration of extension and compression of the association bonds (ν_1 in Fig. 1) and from this frequency to calculate the force constant by means of the familiar relation

$$2K=4\pi^2\nu^2\mu=2\pi^2\nu^2M, \qquad (1)$$

where M is the mass of the monomer.

From the total dimer entropy the contributions of translation and rotation are subtracted to give the internal entropy. It is then assumed that the internal entropy of the monomer is not appreciably changed by combination into the dimer, so that the dimer internal entropy is the sum of twice the monomer internal entropy plus the entropy of six vibrations dependent upon the strength of the association bonds. These vibrations are illustrated in Fig. 1. For all the monomer frequencies except the rotational motion of the hydroxyl group this assumption is acceptable without comment. Extension to include the torsional motion follows at once from the already low entropy (0.75 in formic acid) which could only be further lowered to a minor extent by the restrictive forces resulting from the dimerization.

Table I shows the quantities used to obtain the entropy of the association frequencies. The monomer internal entropy of both acids appears in the first two rows, with the value for hydroxyl torsion set in each case at 0.75, as originally calculated for formic acid, because of the relatively high probable error in the corresponding quantity (1.2) in the acetic acid calculation. This choice has no effect on the conclusions reached in this paper. The first four rows in the dimer summation in the lower part of the table contain the translational and external rotational entropy, with the constant adjusted to permit direct substitution of the monomer weight in grams for M and of 10^{38} times the principal moments of inertia in c.g.s. units for A, B, and C. σ is the symmetry number.

A model based upon the original structure proposed by Pauling and Brockway,[2] rather than the newer and less symmetrical one found by

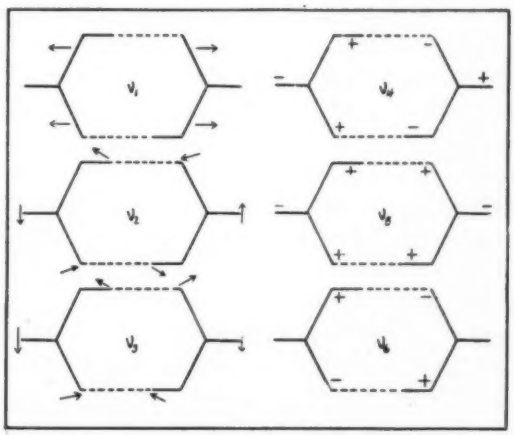

FIG. 1. Vibrations of the formic acid dimer.

[1] J. O. Halford, J. Chem. Phys. 9, 859 (1941); 10, 582 (1942).

[2] L. Pauling and L. O. Brockway, Proc. Nat. Acad. Sci. 20, 336 (1934).

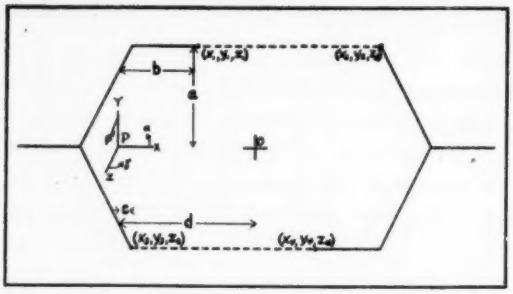

FIG. 2. Coordinates and distances in the formic acid dimer.

Karle and Brockway,[3] is used to calculate the principal moments of inertia. The rotational entropy does not vary appreciably with minor changes in the model. Dimensions used are (H−C)=1.09, (C−O)=(C=O)=1.28, and (C−C)=1.54A units, with the O−C−O angle set at the rounded value of 120°. The oxygen atoms of the individual monomer units are taken to be linked through the bonding hydrogen at a distance of 2.67A units, with the hydrogen atom placed at 1.00 unit from the nearer oxygen. For the principal axes it is accurate enough to take the common bisector of the two O−C−O angles and its perpendiculars in and at right angles to the molecular plane. The two axes in the molecular plane are thus placed slightly out of their true positions because of the location of the hydroxyl hydrogens.

By analogy to the properties of ordinary valence bonds, ν_1 and ν_3 should represent considerably higher frequencies than the remaining four vibrations. It is safe to assume therefore that the entropy of the first frequency is less than one-sixth of the total shown in Table I for the association vibrations. Thus S_1 is less than 2.53 e.u. for formic acid, and, from the Einstein function, ν_1 is greater than 162 cm^{-1}. The corresponding value for K is 1.7×10^4 dynes/cm. Similarly, for acetic acid, S_1 is less than 3.09, ν_1 is greater than 121, and K is above 1.1×10^4. The minimum is therefore determined by the more accurate formic acid entropy.

The probable value is considerably larger because at least one of the bending motions would be expected to have a much larger entropy, leaving less for ν_1. It is more difficult to estimate a maximum. From symmetry considerations ν_1 should be active in Raman scattering but there is no way of predicting how intense the effect should be. It seems improbable, even if the intensity is low, that the Raman line would have escaped detection if the frequency were greater than 250 cm^{-1}, for which K for formic acid is 4.2×10^4. For acetic acid the constant derived from this frequency would be higher.

The result of this estimate, $K=3.0\pm1.3\times10^4$, can be supported in two independent ways, and, in addition, by a more detailed interpretation of the entropy by means of the normal coordinate method. A Raman band has been reported for liquid formic acid at 180±135 by Edsall,[4] at 200 by Kohlrausch, Koppl, and Pongratz,[5] and at 197 cm^{-1} by Morino and Mizushima.[6] According to Hibben[7] this may be analogous to a similar scattering observed for water, for which he suggests as a possible cause a hindered rotation in the liquid state. It is also possible that the effect may be due to the vibrations under discussion here. If so, a frequency of 200 cm^{-1} would indicate for the hydrogen bond a stretching force constant of 2.7×10^4 dynes/cm.

A second independent supporting estimate is based upon the assumption that the ratio of force constant to energy of dissociation is about the same for the association bond as for ordinary hydrogen valence bonds. For the CH, OH, ClH,

TABLE I. Entropy of association vibrations at 25°C.

	Formic acid	Acetic acid
	Monomer	
Vibration	0.60	3.60
Hydroxyl torsion	.75	.75
Methyl torsion	—	2.99
Internal entropy	1.35	7.34
	Dimer	
Constant	49.87	49.87
$\frac{3}{2}R\ln 2M$	13.48	14.27
$\frac{1}{2}R\ln ABC$	3.22	5.04
$-R\ln\sigma$	−1.38	−1.38
Internal, monomer	2.70	14.68
Association bonds	15.21	18.56
	83.10	101.04

[3] J. Karle and L. O. Brockway, J. Am. Chem. Soc. **66**, 574 (1944).

[4] J. T. Edsall, J. Chem. Phys. **4**, 1 (1937).

[5] K. W. F. Kohlrausch, F. Koppl, and A. Pongratz, Zeits. f. physik. Chemie **21B**, 242 (1933).

[6] Y. Morino and S. Mizushima, Sci. Pap. Inst. Phys. Chem. Research (Tokyo) **32**, 33 (1937).

[7] J. H. Hibben, *The Raman Effect and Its Chemical Applications* (Reinhold Publishing Corporation, New York, 1939), p. 180.

TABLE II. Molecular constants of monomer units.

	Formic acid	Acetic acid
$10^{22}M$	0.7593	0.9906
$10^{38}D$	0.7906	1.6053
$10^{38}E$	0.6685	0.7214
$10^{38}F$	0.1221	0.9365
$10^{8}a$	1.109	1.109
$10^{8}b$	1.183	1.675
$10^{8}c$	0.183	0.675
$10^{8}d$	1.518	2.010

TABLE III. Equations for association frequencies.

$10^{-23}\lambda$ (formic acid)	$10^{-23}\lambda$ (acetic acid)
$5.268K$	$4.038K$
$2.497k$	$2.900k$
$6.223K+3.625k$	$3.065K+4.063k$
$21.941k$	$5.645k$
$26.605k$	$9.593k$
$4.228k$	$4.193k$

and BrH bonds this ratio has an average value near 5.7 dynes/cm/cal. The heat of dissociation of the formic acid dimer, 7150 cal. per hydrogen bond, is taken to be near enough to the energy of dissociation and is multiplied by the above ratio to give $K=4.1\times10^4$.

Finally, to provide support for the assumption that the entropy of ν_1 should be considerably less than the average for the six association frequencies, a normal coordinate treatment is undertaken to determine what spread of frequencies is consistent with a simplified but reasonable potential function. In addition to its application to the present problem, this study of a planar system with a center of symmetry but no other symmetry elements is of interest for itself.

The molecular model is shown in Fig. 2 which gives part of the symbolism including the coordinates applied to one monomer unit in setting up the initial equations. Because it has been assumed that the association vibrations are independent of other molecular motions, the model consists of two rigid bodies vibrating against each other. For such a system the kinetic energy may be conveniently expressed in terms of the translation and rotation of the individual rigid bodies. X, Y, and Z represent linear displacements of the centers of mass, while α, β, and γ are angular displacements about the principal axes.

The kinetic energy is given by the following equation:

$$2T=M(\dot{X}_1^2+\dot{Y}_1^2+\dot{Z}_1^2+\dot{X}_2^2+\dot{Y}_2^2+\dot{Z}_2^2)+D(\dot{\alpha}_1^2+\dot{\alpha}_2^2)+E(\dot{\beta}_1^2+\dot{\beta}_2^2)+F(\dot{\gamma}_1^2+\dot{\gamma}_2^2). \quad (2)$$

Subscripts distinguish the two monomer units. D, E, and F are moments of inertia about the axes PZ, PX, and PY, respectively, of Fig. 2.

For the potential energy,

$$2V=K[(x_1-x_2)^2+(x_3-x_4)^2]+2k(y_1^2+y_2^2+y_3^2+y_4^2+z_1^2+z_2^2+z_3^2+z_4^2). \quad (3)$$

Here the subscripts indicate the terminal points of the association bonds, with even numbers applying to one monomer unit and odd numbers to the other, as shown in Fig. 2. To obtain Eq. (3) the general quadratic potential function has been simplified by eliminating all cross products except the x_1x_2 and x_3x_4 terms and reducing the number of constants to two. For this form, K is evidently the stretching valence force constant, while k, which is concerned with lateral displacements, must be a bending force constant. Bending constants defined in this way are about one-fifth to one-tenth as large as stretching constants, and may be converted to angular valence force constants by multiplying by the squares of the appropriate bond lengths. When, as in the present problem, the same constant is used for all the angular displacements, the factor required for this conversion is not evident, and the relation to any specific angular valence force constant is not definite. The product $k(b^2+c^2)$ in Eqs. (7) and (8) should have about the right magnitude for an angular valence force constant because b and c are of the correct order for interatomic distances. Equations (8) show the correct form for the angular vibration between like rotators with the reduced moment of inertia $D/2$, etc. These solutions were put into this form by introducing the factor $2k$ rather than k into Eq. (3).

Six of the twelve coordinates in the kinetic energy equation are eliminated by means of the following linear and angular momentum conditions:

$$\begin{aligned} \dot{X}=\dot{X}_1=-\dot{X}_2 \qquad & \dot{\beta}=\dot{\beta}_1=-\dot{\beta}_2 \\ \dot{Y}=\dot{Y}_1=-\dot{Y}_2 \qquad & 2Md\dot{Y}=D(\dot{\alpha}_1+\dot{\alpha}_2) \\ \dot{Z}=\dot{Z}_1=-\dot{Z}_2 \qquad & 2Md\dot{Z}=F(\dot{\gamma}_1+\dot{\gamma}_2). \end{aligned} \quad (4)$$

The substitutions $\alpha_1=\theta_1+\theta_2$, $\alpha_2=\theta_1-\theta_2$, $\gamma_1=\varphi_1+\varphi_2$ and $\gamma_2=\varphi_1-\varphi_2$ are then made, leading to the expression

$$2T=2M\dot{X}^2+2D(1+D/Md^2)\dot{\theta}_1^2+2D\dot{\theta}_2^2+2E\dot{\beta}^2+2F(1+F/Md^2)\dot{\varphi}_1^2+2F\dot{\varphi}_2^2. \quad (5)$$

TABLE IV. Trial solutions.

ν/ν_1	ν (cm^{-1})	S_{298}
Formic acid, $K=5k$		
1.000	229	1.89
0.308	71	4.13
1.148	263	1.65
0.913	209	2.06
1.005	229	1.89
0.401	92	3.62
$K=3.5\times10^4$		15.24
Formic acid, $K=10k$		
1.000	293	1.46
0.218	64	4.35
1.118	328	1.28
0.645	189	2.24
0.711	208	2.06
0.283	83	3.82
$K=5.7\times10^4$		15.21
Acetic acid, $K=5k$		
1.000	193	2.21
0.379	73	4.07
0.980	189	2.24
0.529	102	3.42
0.689	133	2.91
0.456	88	3.70
$K=3.3\times10^4$		18.55
Acetic acid, $K=10k$		
1.000	246	1.76
0.268	66	4.27
0.927	228	1.89
0.374	92	3.61
0.482	120	3.11
0.322	79	3.92
$K=5.3\times10^4$		18.56

For the transformation of the potential energy the required equations are

$$\begin{aligned} x_1&=X-a\alpha_1 & y_1&=b\alpha_1 & z_1&=a\beta+b\gamma_1\\ x_2&=-X-a\alpha_2 & y_2&=-c\alpha_2 & z_2&=-a\beta-c\gamma_2\\ x_3&=X+a\alpha_1 & y_3&=c\alpha_1 & z_3&=-a\beta+c\gamma_1\\ x_4&=-X+a\alpha_2 & y_4&=-c\alpha_2 & z_4&=a\beta-b\gamma_2, \end{aligned} \tag{6}$$

together with the definition equations for θ_1, θ_2, φ_1, and φ_2. After the transformation the potential energy has the form

$$\begin{aligned} 2V=&8KX^2+4k(b^2+c^2)(\theta_1^2+\varphi_1^2+\varphi_2^2)\\ &+4[2Ka^2+k(b^2+c^2)]\theta_2^2\\ &+8ka(b-c)\beta\varphi_2+8ka^2\beta^2. \end{aligned} \tag{7}$$

The solutions for $\lambda=4\pi^2\nu^2$ for the first four vibrations of Fig. 1 take the forms

$$\begin{aligned} &\lambda_1=4K/M \qquad \lambda_2=2k(b^2+c^2)/[D(1+D/Md^2)]\\ &\lambda_3=[4Ka^2+2k(b^2+c^2)]/D \qquad\qquad (8)\\ &\lambda_4=2k(b^2+c^2)/[F(1+F/Md^2)]. \end{aligned}$$

For λ_5 and λ_6,

$$\begin{vmatrix} E\lambda-4ka^2 & -2ka(b-c) \\ -2ka(b-c) & F\lambda-2k(b^2+c^2) \end{vmatrix}=0. \tag{9}$$

The masses, moments of inertia, and distances required for numerical solution of the above equations are collected in Table II. The moments D, E, and F have been calculated with the aid of the dimensions listed earlier for the dimer and are subject to a similar but relatively larger error because of the deviation of the selected rotational axes from the principal axes. The error is again taken to be negligible. The distances a, b, and c are coordinates referred to the axes PX and PY, as shown in Fig. 2, and d is the distance between O, the center of mass of the dimer, and P, that of the monomer unit.

Substitution of the constants of Table II into Eqs. (8) and (9) yields the simplified expressions of Table III.

In principle the two potential constants could be found by trial from the two entropy totals of Table I, but the result so obtained would have little meaning because of the relatively large uncertainty in the acetic acid entropy. It seems better to assign a reasonable value to K/k, to evaluate from this the ratios λ/λ_1 and ν/ν_1, and to find by trial from the entropy-frequency curve a set of frequencies in the corresponding ratios which will yield the correct entropy. Table IV shows in successive columns the frequency ratios, the frequencies, and the entropy summation for four such trial solutions.

The assumed ratios of 5 and 10 for K/k are of the order usually found for ordinary valence bonds. For each ratio the spread of the calculated frequencies is several-fold and ν_1 appears at or near the maximum, accounting for considerably less than one-sixth of the entropy of the association frequencies. It is therefore probable that ν_1 for formic acid lies in the region between 200 and 250 cm^{-1} and that K is not far from 4×10^4 dynes/cm.

In the absence of a more accurate method of evaluation this provides a satisfactory approximation to the stretching potential constant of the association bond in the carboxylic acid dimer.

Letters to the Editor

THIS section will accept reports of new work, provided these are terse and contain few figures, and especially few halftone cuts. The Editorial Board will not hold itself responsible for opinions expressed by the correspondents. Contributions to this section should not exceed 600 words in length and must reach the office of the Managing Editor not later than the 15th of the month preceding that of the issue in which the letter is to appear. No proof will be sent to the authors. The usual publication charge ($3.00 per page) will not be made and no reprints will be furnished free.

New Units for the Measurement of Radioactivity

E. U. CONDON AND L. F. CURTISS
National Bureau of Standards, U. S. Department of Commerce, Washington, D. C.
May 20, 1946

IT has become the custom to express the strength of radioactive sources in terms of curies. This is an erroneous use of this unit since by original definition the curie is that "amount of radon in equilibrium with one gram of radium"[1] as defined by the Radiology Congress in Brussels in 1910. Therefore, the curie can be used only to represent a rate of disintegration in the radium family. It then represents the disintegration rate of radium or its products in equilibrium. Such a use has been indorsed by the International Radium Commission.

The quantity to be specified in designating the strength of radioactive sources in general is the disintegration rate, determined by the decay constant and the number of atoms of the radioactive isotope in the source. This is simply a number, and therefore to establish a suitable unit the only requirement is to select a convenient number of disintegrations per second and give it a name. In selecting this number, consideration should be given to insure that it can be readily expressed in sub-multiples and multiples by the usual prefixes, kilo, milli, micro, etc. A number which fits this requirement is 10^6. Since the curie was named in honor of M. and Mme. Curie, the co-discoverers of radium, it is natural to select the name "rutherford" for the new unit. The appropriate abbreviation is "rd," which conflicts with the abbreviation of no other well accepted physical unit. The micro-rutherford would become one disintegration per second, a convenient number to remember. Furthermore, the rutherford itself is a small unit of the order of magnitude of many sources used in laboratory measurements. It is sufficiently different in size from the curie that no confusion can arise with the curie in connection with measurements of activities in the radium family. Large sources would require the use of positive powers of ten, which would be preferable to the use of a large unit requiring negative powers of ten.

It should be pointed out that the continued use of the curie for all radio-isotopes not only requires a redefinition of the curie, but in addition the value of the curie is uncertain to at least 4 percent and values are in current use well outside this limit. The rutherford provides a definite unit. In addition to eliminating the undesirable use of the curie, the proposed unit also eliminates the basic necessity for measuring radio-isotopes in terms of a standard. Any measuring device which will determine the total number of disintegrations per second will provide directly the strength of the source in rutherfords. A counting arrangement for which the solid angle factor is known is an example. Radioactive standards may be used to determine this factor for a given geometrical arrangement, but other methods are also available.

In the measurement of sources of gamma rays, the roentgen has gained increasing use, largely because this unit is independent of the quality (electron volts) of the gamma radiation. There is need for a unit in which the intensity of gamma-ray sources can be expressed to eliminate the use of the curie for this purpose. An obvious unit derived from the definition of the roentgen is a roentgen-per-hour at one meter. The roentgen-per-hour at one meter can be abbreviated r.h.m., which again is not readily confused with any other common abbreviation. It has been suggested that this abbreviation can be pronounced "rum." It should be noted that a gamma-ray source equal to one r.h.m. will have a gamma-ray strength 1.18 times that of 1 curie of radium. Therefore, the roentgen-per-hour at one meter has the same order of magnitude as the curie in the measurement of gamma-ray sources.

The National Bureau of Standards, at the suggestion of the Committee on Radioactivity of the National Research Council, recommends the general use of these units.

[1] E. Rutherford, "Radioactive Substances and Their Radioactivity" (1913), p. 479. "The Radioactive Constants as of 1930," International Radium-Standards Commission Report, Rev. Mod. Phys. **3**, 427 (1931).

The Electron Affinity of Amide Radical and the Chemical Stability of Metal-Ammonia Solutions

RICHARD A. OGG, JR.
Department of Chemistry, Stanford University, California
May 13, 1946

NEW experimental studies have been carried out, dealing with concentration and temperature dependence of electrical conductivity and of the near ultra-violet absorption spectrum of liquid ammonia solutions of sodium and potassium amides. These substantiate older observations[1] that the amides behave as weak electrolytes, and indicate that the dissociation constants increase with rising temperature. They also show that the constituent responsible for the yellow color of such solutions is the amide ion, NH_2^-. Of particular importance is the observation that light absorption by the amide ion results in a striking photo-conductivity. This fact supports the interpretation of the observed continuous absorption spectrum as an *electron affinity spectrum*,[2] corresponding to the physical process

$$NH_2^-(NH_3)+h\nu \rightarrow NH_2(NH_3)+e(NH_3).$$

No over-all photochemical reaction is observed, suggesting

that recapture of conduction electrons by the free amide radicals must be rapid.

The long wave-length threshold of the amide ion light absorption is at about 4200A, corresponding to an energy of some 68 kilocalories per mole. This value would appear to represent a *numerical upper limit* for the energy change associated with the above dissociation process. Some related considerations employing Hess' law are of paramount importance in understanding the remarkable chemical stability of metal-ammonia solutions. In the following equations, the inequality signs refer to *algebraic* values of the corresponding reaction energies, given in kilocalories per mole:

$$NH_3(g) \rightarrow NH_2(g)+H(g) \qquad E_1 < -84, \quad (1)$$
$$NH_2(g) \rightarrow NH_2(NH_3) \qquad E_2 \sim +6, \quad (2)$$
$$NH_3(l) \rightarrow NH_3(g) \qquad E_3 \sim -6, \quad (3)$$
$$H(g) \rightarrow H(NH_3) \qquad E_4 \sim 0, \quad (4)$$
$$e(NH_3)+NH_2(NH_3) \rightarrow NH_2^-(NH_3) \qquad E_5 < +68, \quad (5)$$

$$e(NH_3)+NH_3(l) \rightarrow NH_2^-(NH_3)+H(NH_3) \qquad E_6 < -16. \quad (6)$$

Reaction (6), being endothermic by at least 16 kilocalories, must have an activation energy at least as great as this value. Since the dissociation energy of the "first" N−H bond in NH_3 is without doubt greater numerically than the average value[3] used for reaction (1), a more probable estimate of the minimum activation energy of (6) would be of the order of 30–40 kilocalories per mole. That such large values actually obtain is indicated by the author's observations that highly purified metal-ammonia solutions preserved in sealed vessels at room temperature require several months for practically complete discharge of the characteristic blue color. The probable role of catalysts is to lower the energy deficit of reaction (6) by adsorption of hydrogen atom. In support of this postulate is the fact that the metals most suitable for hydrogenation catalysts are also the most effective in promoting amide formation in metal-ammonia solutions.

If the far ultraviolet absorption spectrum of aqueous hydroxyl ion[4] is interpreted as an electron affinity spectrum, entirely analogous considerations indicate the reaction

$$e(aq)+H_2O(l) \rightarrow OH^-(aq)+H(aq)$$

to be considerably *exothermic* and hence probably associated with a negligible activation energy. This affords a ready explanation of the impossibility of preparing aqueous metal solutions containing "solvated" electrons, and suggests that affinity spectra of aqueous negative ions should not be attended by photo-conductivity.

If the solvation energy of conduction electrons in ammonia is estimated as less than 10 kilocalories,[5] then the numerical upper limit for the sum of the electron affinity of amide radical and the solvation energy of amide ion in ammonia is roughly 68+6+10=84 kilocalories. Any reasonable estimate of the amide ion solvation energy results in an extremely small electron affinity for the amide radical—of the order of 20–30 kilocalories. Such a value would fall in logical sequence with the respective figures of 95 and 48 kilocalories for the electron affinities[3] of F and OH. So small a value for the electron affinity of amide radical, as compared with the ionization potentials of alkali metal atoms, would suggest that the binding in the alkali metal amides is predominantly *covalent*. The experimentally observed weak electrolyte behavior in liquid ammonia solution supports this view, as do the relatively high volatibility and low melting points of the pure substances.[6]

[1] C. A. Kraus, *The Properties of Electrically Conducting Systems* (Chemical Catalogue Company, 1922).
[2] J. Franck and G. Scheibe, Zeits. f. physik. Chemie **A139**, 22 (1928).
[3] O. K. Rice, *Electronic Structure and Chemical Binding* (McGraw-Hill Book Company, Inc., New York, 1940).
[4] H. Ley and B. Arends, Zeits. f. physik. Chemie **B6**, 240 (1929).
[5] R. A. Ogg, Jr., J. Chem. Phys. **14**, 295 (1946).
[6] F. W. Bergstrom and W. C. Fernelius, Chem. Rev. **12**, 43 (1933).